J. Fluid Mech. (1988), *vol.* 188, *pp.* 223–252
Printed in Great Britain

Subharmonic resonance, pairing and shredding in the mixing layer

By PETER A. MONKEWITZ

Department of Mechanical, Aerospace and Nuclear Engineering, University of California, Los Angeles, CA 90024, USA

(Received 4 March 1987)

An instability-wave analysis is presented to describe the spatial evolution of a fundamental mode and its subharmonic on an inviscid parallel mixing layer. It incorporates explicitly the weakly nonlinear interaction between the two modes. The computational finding that the development of the subharmonic, leading eventually to pairing or shredding, crucially depends on its phase relation with the fundamental is fully confirmed. Furthermore it is shown that a critical fundamental amplitude has to be reached before the (spatial) subharmonic becomes phase locked with the fundamental and exhibits a modified growth rate. Then the analysis is exploited to explain the occurrence of amplitude modulations in 'natural' mixing layers and to estimate the width of the subharmonic spectral peaks. Also, the case of oblique subharmonic waves is briefly touched upon. In the last part, ways are explored to model non-parallel effects, i.e. to handle the saturation of the rapidly growing subharmonic. Using this wave description, the role of mode interaction in the 'vortex pairing' and 'shredding' process is assessed.

1. Introduction

The experimental studies directly or indirectly concerned with the interaction of 'coherent structures', and in particular with 'vortex pairing' in the mixing layer, have reached now such a number that their enumeration is beyond the scope of this introduction. So only the early works of Wehrmann & Wille (1958), Brown & Roshko (1974) and Browand & Weidman (1976) are mentioned here; for an extensive recent review of the subject, the paper by Ho & Huerre (1984) may be consulted.

A common characteristic of all the experiments is that many results are quite accurately predicted by simple, locally parallel linear stability theory. Most prominent among these features are the passage frequency of 'fully rolled up coherent structures' and their spacing or phase velocity. Even the shapes of the disturbance velocity and vorticity profiles are often predicted with astonishing detail even in regions around saturation where the nonlinear roll-up of the initially linear instability wave is complete! This leads naturally to the question of why linear or 'minimally nonlinear' stability theory is so successful in the mixing layer, where disturbance levels are high and nonlinearities are thought to be prevalent. It is this question that provides the main motivation for the following study, which focuses in particular on the interaction between a fundamental and its subharmonic disturbance. To fix ideas, the mixing layer under study is sketched in figure 1, which also serves to define the coordinate system and the velocity ratio R.

It is clear that nonlinearity has to be introduced in some form to handle mode interactions and the saturation of an instability wave. The different known ways of

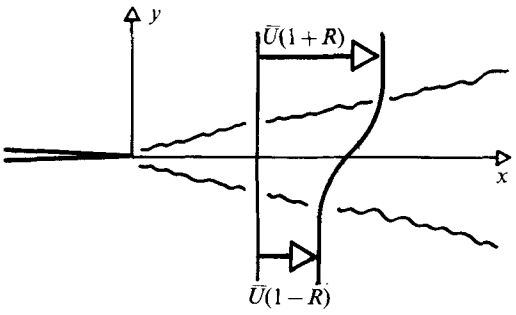

FIGURE 1. The mixing layer under consideration.

doing this are briefly reviewed in the remainder of this section. First, cases are considered where the evolution of only one mode is followed. In order to predict saturation amplitudes, the weakly nonlinear approach of Stuart (1960) and Watson (1960) can be used, which is inherently restricted to modes close to neutral. For such cases it has been applied extensively to the mixing layer by Huerre (1987), Churilov & Shukhman (1987) and Maslowe (1977), for instance. The latter author has concentrated on the stratified mixing layer, where near neutrality can be obtained by a suitable choice of Richardson number. In all homogeneous mixing layers, however, disturbances start as approximately maximally amplified modes, i.e. far from neutral, where, owing to the inviscid inflexion point instability, they grow very rapidly. Therefore an amplitude expansion patterned after the weakly nonlinear formulation would in this case only yield non-resonant corrections to the result of linear theory, and would be unable to predict saturation.

The 'slowly diverging' linear stability analysis, on the other hand, which originated from work of Bouthier (1972), has been more successful in predicting the amplitude evolution in mixing layers and jets, as shown by Crighton & Gaster (1976). The method was first used to take into account the viscous growth of the Blasius boundary layer. Its application to inviscidly unstable flows, on the other hand, requires a different interpretation. The discussion in the following is restricted to the mixing layer, which is known to spread (on the average) linearly with downstream distance. Except in an initial region, where disturbance levels are low, its divergence can therefore clearly not be attributed to the action of molecular viscosity alone. Introduction of an 'eddy viscosity' proportional to x, as Görtler (1942) proposed, does indeed confirm the linear spreading, but the 'mixing length' associated with this eddy viscosity turns out to be of the order of the mixing-layer thickness. Hence the 'eddies' essentially represent the dominant instability wave and it appears that small-scale turbulence – less the 'large-scale structures' – cannot account for the growth of the mixing layer. The work of Liu & Merkine (1976), and others, who studied the interaction of instability waves and fine-grained turbulence with an energy method, confirms this point. Therefore it must be concluded that the spreading of the mixing layer is mostly a nonlinear effect, i.e. due to 'mean flow correction' in weakly nonlinear terminology. The slowly diverging linear approach should in this case really be called the 'method of anticipated mean-flow correction'. Significantly, the mean-flow divergence is introduced at an earlier stage – to be precise, two orders in the disturbance amplitude earlier – than it appears in standard weakly nonlinear theory. Accordingly, the method must be considered more than weakly nonlinear, which makes it generally incompatible with a standard weakly

nonlinear approach to mode interactions. The success of the slowly diverging approach has been demonstrated experimentally by, among others, Gaster, Kit & Wygnanski (1985), who used measured mean-velocity profiles to accurately predict the evolution of a single mode. The 'slightly diverging' approach introduced by Huerre & Crighton (1983) also falls into this same class of methods. It introduces the flow divergence at linear order in the disturbance amplitude and is, therefore, located in terms of 'nonlinearity' between the slowly diverging and the weakly nonlinear approach. In §4 this method will be further discussed and incorporated in the model.

As soon as more than one mode is present in the mixing layer, the main interest is in their interaction. While Robinson (1973) studied non-resonant interactions, this paper will only be concerned with the 'dramatic' resonant interaction relating to 'vortex pairing' and 'shredding'. The modelling of these phenomena has been approached both numerically and analytically. The numerical work of Patnaik, Sherman & Corcos (1976), Acton (1976), Riley & Metcalfe (1980), Corcos & Sherman (1984), and others, has all been concerned with temporally growing, i.e. spatially periodic mixing layers, while only a few studies, notably by Ashurst (1979) and more recently by Mansour & Barr (1987) and others, have dealt with the spatially developing mixing layer. The analytical work has been initiated by von Kármán & Rubach (1912) who studied the stability of different arrangements of point vortices, and found then that the most dangerous instability of a single row of equal vortices is the subharmonic. Then, Kelly (1967) was the first to study the subharmonic instability in the presence of a fundamental with distributed vorticity. His temporal analysis predicted that the interaction would be most pronounced when the fundamental is close to the linearly neutral mode. It also implicitly predicted the strong dependence of the interaction on the phase relation between fundamental and subharmonic (Monkewitz 1982) in complete agreement with the numerical calculations mentioned above. The confirmation of Kelly's work by Pierrehumbert & Widnall (1982), who studied secondary instabilities on 'Stuart-vortices' (Stuart 1967), is noted in passing. Amplitude equations resulting from subharmonic resonance have also been explored in a more formal way by Redekopp (1977).

The plan of the present paper is as follows. In §2, Kelly's weakly nonlinear way of handling the mode interactions is adapted to instability waves which develop spatially on a parallel hyperbolic-tangent mixing layer. Conditions are established for resonant interaction between a fundamental–subharmonic pair, and amplitude equations for the fundamental and the subharmonic are derived. In §3, results of this (locally) parallel analysis are presented.

Then, in §4, a heuristic model is developed which, in addition to the fundamental–subharmonic interaction, also incorporates the effect of slight flow divergence. With this, it is possible to follow the subharmonic all the way to saturation and to 'produce' a complete pairing interaction. Finally, in §5 the results of this study are assessed and used to give an interpretation of 'vortex pairing' and 'shredding' in terms of vorticity, viz. instability waves.

2. The instability-wave analysis for a parallel mixing layer

In this analysis a parallel mixing layer is considered, which is disturbed at a fundamental frequency and its subharmonic, i.e. at half the fundamental frequency. Both disturbances are thereby represented by spatially developing instability waves. As will be shown below in detail, the situation of particular interest, which is that of

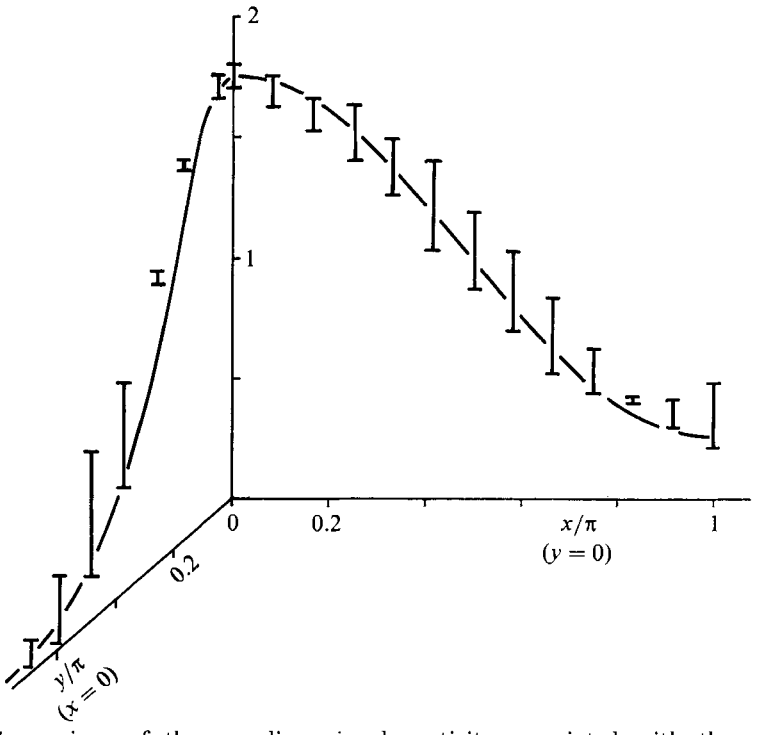

FIGURE 2. Comparison of the non-dimensional vorticity associated with the superposition $\psi^{(0)}+\alpha\psi^{(\alpha)}$ (see (2.2) and (2.6)) of mean flow and neutral fundamental (solid line, using $A \equiv 1$ and $\alpha = 0.1875$) and the vorticity distribution measured by Browand & Weidman (1976). The bars represent the experimental asymmetry of the structure.

resonance between fundamental and subharmonic, occurs where the fundamental is neutrally stable on a linear basis. On a real spatially developing mixing layer this location approximately coincides with the saturation location of the fundamental (see e.g. Ho & Huerre 1984). Hence, the physical phenomenon addressed here is the interaction between a spatial instability wave (the fundamental) and its subharmonic in a neighbourhood of the downstream station where the fundamental reaches maximum amplitude.

In order to arrive at a consistent mathematical formulation in this section, several simplifying assumptions are made. The first is the assumption of a *parallel mean flow*, which may be justified by the experimental finding that highly organized (forced) mixing layers are approximately locally parallel around the saturation location of each mode in a subharmonic sequence (Ho & Huerre 1984, figure 24). A second simplification, already mentioned above, is achieved by describing the *fundamental* as a *linear neutral wave*. The connection with the experiment may be established by noting the excellent correspondence between the measured vorticity of a phase-averaged 'large-scale structure' (Browand & Weidman 1976) and the simple linear superposition of mean vorticity and the vorticity associated with such a linear neutral disturbance of suitably adjusted amplitude (see figure 2). These measurements are also noted by Corcos & Sherman (1984) to be in excellent agreement with their numerical simulations (presumably after smoothing of the fine detail in their finite-amplitude billow). It must be said, however, that the magnitude of the fundamental amplitude used in figure 2 does strain the limitations of the theory that is developed below.

2.1. *Formulation of the problem*

To further simplify the problem, compressibility and viscous effects are neglected and the interaction between the two instability waves is assumed to be weak. Hence the total stream function is expanded, as in weakly nonlinear theory, in powers of α and β, two small parameters characterizing the fundamental and subharmonic amplitudes respectively. The weakest possible restrictions on α and β which are necessary for mathematical consistency and the relevance of the theory will be discussed below. Keeping only terms up to quadratic order, one has

$$\psi = \psi^{(0)} + \alpha\psi^{(\alpha)} + \beta\psi^{(\beta)} + \alpha^2\psi^{(\alpha\alpha)} + \alpha\beta\psi^{(\alpha\beta)} + \beta^2\psi^{(\beta\beta)} + O(\alpha^3, \ldots). \tag{2.1}$$

The zeroth-order term $\psi^{(0)}$, given below in terms of streamwise velocity, represents the mean flow, and is at this point chosen to be a parallel hyperbolic-tangent mixing layer,

$$\psi_y^{(0)} = 1 + R\tanh y. \tag{2.2}$$

The reference velocity for the above non-dimensional expression is the average velocity $\bar{U}$ between the two streams, and R is the velocity ratio defined as $R = \Delta U/2\bar{U}$ with ΔU the velocity difference between the two streams. The reference length implicit in (2.2) is one half the vorticity thickness of the layer, which is the same as twice the momentum thickness for the hyperbolic-tangent profile.

When focusing on the interaction between the fundamental $\psi^{(\alpha)}$ and its subharmonic $\psi^{(\beta)}$, situations with the strongest, resonant, interactions are of primary interest. That is, conditions are sought where the linear modes are themselves modified by interactions, while the additive quadratic corrections $\psi^{(\alpha\alpha)}$ etc. are only of secondary importance. These resonance conditions arise when, formally speaking, the straightforward solution of the inhomogeneous equations governing the quadratic contributions to the stream function produces secular terms, i.e. when an interaction term reproduces the x–t (downstream distance–time) dependence of either linear mode. The interaction of particular interest here occurs at order $\alpha\beta$, where the inhomogeneous term involving products of $\psi^{(\alpha)}$ and $\psi^{(\beta)}$ resonates with the subharmonic $\psi^{(\beta)}$. In the terminology of the multiple-scales approach, which will be adopted here, this particular case of parametric resonance results in the subharmonic at leading-order β being modified by the presence of the fundamental on the slow space and/or timescales

$$\hat{x} = \alpha x, \quad \hat{t} = \alpha t. \tag{2.3}$$

Such a resonance, however, can only occur under the following conditions: (i) the frequency ratio of the modes (α) and (β) is approximately 2 to 1; (ii) their real phase speeds are sufficiently close to allow a sustained interaction; and (iii) the sum of their growth rates is approximately equal to the growth rate of the subharmonic alone. This last condition is necessary because in a homogeneous mixing layer growth rates cannot in general be considered as small. While this is obvious at a velocity ratio R of unity, where the maximum spatial amplification over one wavelength is by a factor of about 30, it will be shown below that the same arguments apply for all R compatible with this approach.

Upon inspection of the linear stability diagram, reproduced in figure 3, the conditions (i)–(iii) immediately narrow the choice of the two modes to a *fundamental close to neutral* and a *subharmonic close to maximally amplified*. This is the only case where a resonant interaction between the two modes can occur. The situation is no different in the temporal case considered by Kelly (1967). Although condition (ii),

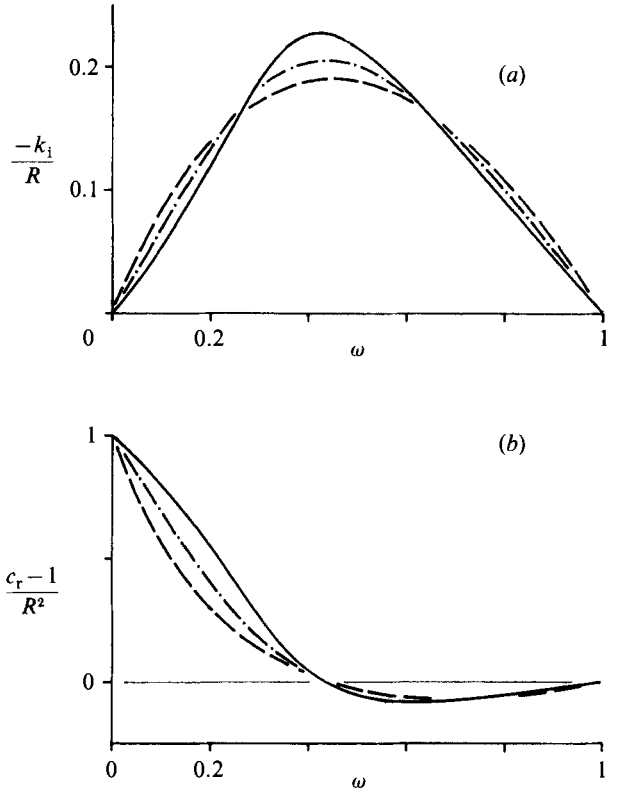

FIGURE 3. (*a*) Spatial amplification rate $-k_i$ normalized by R, and (*b*) real phase velocity $c_r = \omega/k_r$, normalized as $(c_r-1)/R^2$, versus frequency for the hyperbolic-tangent mixing layer (adapted from Monkewitz & Huerre 1982): ——, $R = 1$; –·–, $R = 0.7$; – –, $R \ll 1$.

requiring equality of the real phase speeds, is satisfied for any pair of temporal modes, (iii) again leads to the choice above. It is noted here that Kelly did not enforce condition (iii) in his analysis, although he did consider in his §4 (example 3 of case A) the situation where the fundamental is neutral (cf. his table 1), among other cases where resonance is induced by implicitly assuming small growth rates (cf. also Monkewitz 1982).

Summarizing this discussion, the subharmonic growth rate is considered an order-one quantity, which automatically limits resonances to interactions *linear* in the subharmonic and to self-interactions of the near-neutral fundamental (starting with α^3). In particular, the subharmonic does not react back on the fundamental in a resonant fashion at order β^2, a behaviour which follows here naturally from condition (iii) as opposed to being assumed as in Kelly (1967). As a further consequence, the saturation of the subharmonic is beyond the reach of the present analysis or, in other words, *the evolution of the subharmonic can be corrected for the presence of the fundamental only in the region where, by itself, it would follow linear theory*. In this respect the analysis differs from the classical weakly nonlinear theory which, under the assumption of small growth rates, produces results uniformly valid in space and time. Nevertheless, in the limited region defined above, the present approach can be extended in a rational fashion to any order in α and β.

At this point, the necessary restrictions on the fundamental and subharmonic

amplitudes can be derived. A first condition implicit in the formulation is that both α and β are much smaller than unity. However, there is no need to require *a priori* $\beta \ll \alpha$ as in Kelly (1967). A second limitation becomes apparent when considering the small shear limit $R \to 0$. In this limit, maximum growth rates are small, $O(R)$ (see Monkewitz & Huerre 1982), and hence it is tempting to relax the resonance condition (iii). That this is not permitted can be most easily seen by considering Gaster's transformation, discussed in Monkewitz & Huerre (1982): for small R the leading-order (in R) spatial problem is equivalent to a temporal problem. Hence one can get rid of the average mean velocity by a Galilean transformation and one is left with a disturbance of order α riding on a mean flow of order R. If the ordering implied in (2.1) is to be preserved, one must have $\alpha \ll R$. Therefore, when $R \to 0$, the lengthscale $\hat{x}$ for the interaction of interest increases in the same proportion as the streamwise distance required for the linear growth of the subharmonic.

Furthermore, to have resonance at order $\alpha\beta$, the difference between fundamental and subharmonic phase speed cannot be larger than $O(\alpha)$. This is conveniently expressed in terms of the 'detuning parameter', to be introduced later by way of (2.12), which must be limited to order unity. Noting that this parameter is well approximated by $-(0.03\,R^2)/\alpha$ (see figure 3, and Monkewitz & Huerre 1982), and combining this with the result of the preceding discussion of the small-R limit, one arrives at the constraint (2.4*a*) for α.

Besides requiring mathematical consistency, leading to (2.4*a*), the question of relevance has to be examined as well. As stated above, the analysis is only valid in the region where the subharmonic, by itself, follows linear theory. Its modification by the presence of the fundamental, which is here of interest, requires on the other hand a distance $\Delta\hat{x}$ of order unity (see (2.3)). Therefore, for the theory to yield results of practical relevance, the subharmonic amplitude has to remain small over the distance $\Delta\hat{x} = O(1)$. That is, one has to require $\beta \exp[-k_i \Delta\hat{x}/\alpha] \ll 1$, which leads directly to the constraint (2.4*b*), where $-k_i$ denotes the linear subharmonic growth rate. Otherwise the saturation of the subharmonic, which is not considered here, would dominate over the influence of the fundamental. Thus we require

$$O(0.03\,R^2) \leqslant \alpha \ll R, \tag{2.4a}$$

$$\beta \ll \exp\left[\frac{k_i}{\alpha}\right]. \tag{2.4b}$$

2.2. *The disturbance equations*

Introducing the expansion (2.1) into the Euler equation, with $\psi^{(0)}$ given by (2.2), yields first at linear order the Rayleigh equation for $\psi^{(\alpha)}$ and $\psi^{(\beta)}$, which depend on the fast linear instability variables as well as parametrically on the slow variables (2.3):

$$\left.\begin{aligned} &\mathscr{R}[\psi^{(\alpha,\beta)}(x, y, t; \hat{x}, \hat{t})] = 0,\ \psi^{(\alpha,\beta)} \to 0 \quad \text{as } |y| \to \infty, \\ &\mathscr{R} \equiv \left[\frac{\partial}{\partial t} + \psi_y^{(0)} \frac{\partial}{\partial x}\right] \nabla^2 - \psi_{yyy}^{(0)} \frac{\partial}{\partial x}. \end{aligned}\right\} \tag{2.5}$$

According to the previous discussion, the fundamental has to be close to neutral, with a non-dimensional frequency $\omega^{(\alpha)} = 1 + O(\alpha)$, where a small detuning of order α is allowed. Hence the subharmonic frequency is given by $\omega^{(\beta)} = \frac{1}{2} + O(\alpha)$. Using multiple scales, the deviations from 1 and $\frac{1}{2}$, respectively, are taken up in the

dependence on the slow time (2.3), and the solutions of (2.5), using c.c. for the complex conjugate, can be written as

$$\psi^{(\alpha)} = A(\hat{x},\hat{t})\,\mathrm{sech}\,y\,\exp[\mathrm{i}(x-t)]+\mathrm{c.c.}, \tag{2.6}$$

$$\psi^{(\beta)} = B(\hat{x},\hat{t})\,\phi(y)\,\exp[\mathrm{i}(kx-\tfrac{1}{2}t)]+\mathrm{c.c.} \tag{2.7}$$

The amplitude functions A and B are now determined as usual, at order α^2 and $\alpha\beta$ respectively, by solvability conditions. At order α^2 the amplitude function $A(\hat{x},\hat{t})$ is obtained from (2.8) below, which has already been given by Huerre (1987) and Churilov & Shukhman (1987) under the assumption of a fully viscous critical layer. In other words, nonlinear effects in the critical layer are neglected or, equivalently, the critical layer Reynolds number as defined by $Re_{\mathrm{CL}} = Re\,\alpha^{\frac{3}{2}}$ is assumed to be much smaller than unity, where Re is the Reynolds number based on mixing-layer thickness. This choice is motivated by the observation that, despite sizable disturbance amplitudes, the experimentally determined growth rate slope $\mathrm{d}k_{\mathrm{i}}/\mathrm{d}\omega$ ($\omega = 1$) near the neutral point seems to agree better with viscous rather than nonlinear critical–layer theory (see Ho & Huerre 1984, figure 2; for a discussion of nonlinear effects see their §2.2). We have

$$A_{\hat{x}}+\left[1-\frac{2\mathrm{i}R}{\pi}\right]^{-1}A_{\hat{t}} = 0. \tag{2.8}$$

The factor $[1-2\mathrm{i}R/\pi]$ in (2.8) is easily identified as the (complex) group velocity of the neutral disturbance which arises naturally in the Taylor expansion of $\psi^{(\alpha)}$ around $\omega = 1$. Assuming a small frequency deviation from neutral, $\omega^{(\alpha)} = 1+\alpha\Omega^{(\alpha)}$, which is taken up into the slow scale $\hat{t} = \alpha t$, one has

$$A(\hat{x},\hat{t}) = A_0\exp\left\{\left[1-\frac{2\mathrm{i}R}{\pi}\right]^{-1}\mathrm{i}\Omega^{(\alpha)}\hat{x}-\mathrm{i}\Omega^{(\alpha)}\hat{t}\right\}. \tag{2.9}$$

In the following, A_0 will be set equal to unity, so that α can be directly identified as the maximum amplitude of the streamwise velocity disturbance associated with the fundamental at the location $\hat{x} = 0$ and $y = \pm\ln[1+\sqrt{2}]$.

Next, the order $\alpha\beta$ is considered and the following inhomogeneous equation for $\psi^{(\alpha\beta)}$ is obtained:

$$\left.\begin{aligned}
&\mathscr{R}[\psi^{(\alpha\beta)}] = \sum_{i=1}^{3} H_i^{(\alpha\beta)},\\
&H_1^{(\alpha\beta)} = -\frac{\partial}{\partial\hat{x}}\{2\psi_{\hat{t}x}^{(\beta)}+\psi_y^{(0)}(2\psi_{xx}^{(\beta)}+\nabla^2\psi^{(\beta)})-\psi_{yyy}^{(0)}\psi^{(\beta)}\},\\
&H_2^{(\alpha\beta)} = -\frac{\partial}{\partial\hat{t}}\nabla^2\psi^{(\beta)},\\
&H_3^{(\alpha\beta)} = J(\psi^{(\alpha)},\nabla^2\psi^{(\beta)})+J(\psi^{(\beta)},\nabla^2\psi^{(\alpha)}).
\end{aligned}\right\} \tag{2.10}$$

Above, the shorthand $J(f,g)$ stands for the Jacobian $\partial(f,g)/\partial(x,y)$. The first two $H^{(\alpha\beta)}$ arise from the dependence of $\psi^{(\beta)}$ on the slow scales $\hat{x}$ and $\hat{t}$, while the third H represents the interaction term. This last $H_3^{(\alpha\beta)}$ produces the two frequencies $\omega = 1\pm\frac{1}{2}+O(\alpha)$. Therefore, part of this term will resonate with the subharmonic.

Recalling that the $\psi^{(\alpha)}$ and $\psi^{(\beta)}$ are twice the real part of the complex expressions (2.6) and (2.7), the fast-scale behaviour of the part of $H_3^{(\alpha\beta)}$ with the frequency $+\frac{1}{2}$ is

$$H_3^{(\alpha\beta)} \propto \mathrm{e}^{\mathrm{i}(x-t)}[\mathrm{e}^{\mathrm{i}(kx-\frac{1}{2}t)}]^*, \tag{2.11}$$

where the asterisk is used to indicate the complex conjugate. This can be manipulated to reproduce the fast-scale behaviour of $\psi^{(\beta)}$ as follows:

$$\left.\begin{aligned} x-t-(k_\mathrm{r}-\mathrm{i}k_\mathrm{i})x+\tfrac{1}{2}t = kx-\tfrac{1}{2}t+2\kappa\hat{x}, \\ \kappa \equiv \alpha^{-1}(\tfrac{1}{2}-k_\mathrm{r}) \leqslant O(1). \end{aligned}\right\} \tag{2.12}$$

The above rescaling of the 'leftover' term $(\frac{1}{2}-k_\mathrm{r})x$ is only legitimate when the real phase speed of the subharmonic is close to unity, i.e. to the phase speed of the neutral fundamental. This condition is satisfied by the present choice of modes since for, say, $R = 1$, $(\frac{1}{2}-k_\mathrm{r}) = -0.0274$ at $\omega = \frac{1}{2}$. Thereby the parameter κ determines the degree of detuning of the resonance and will henceforth be referred to as the *detuning parameter*. It is noted here that in the spatial case under consideration no perfect tuning of the subharmonic resonance is possible, since no pair of modes can be found (see figure 3) which simultaneously satisfy exactly all three resonance conditions discussed in the last §2.1.

After this rearrangement of the interaction term, a solvability condition has to be applied to (2.10) which requires that the right-hand side be orthogonal to the solution of the adjoint Rayleigh equation, i.e. to $\{\phi(y)[\psi_y^{(0)}-1/(2k)]^{-1}\}^*$. To compute the ensuing integrals, first the Rayleigh equation is solved for $\phi(y)$ at $\omega^{(\beta)} = \frac{1}{2}$. The eigenfunction is normalized to $\phi(0) = 1$, which yields a maximum non-dimensional amplitude of the streamwise velocity disturbance $|\phi_y(y = -0.06)| = 0.822$. The integrals are then computed numerically by Simpson's rule over the central portion of the mixing layer and analytically outside the computational domain, using asymptotic representations of ϕ (see Monkewitz & Huerre 1982). From this, one obtains the equations for the subharmonic amplitude B and its complex conjugate B^*,

$$B_{\hat{x}}+pB_{\hat{t}}+rA(\hat{x},\hat{t})\,B^*\exp(2\mathrm{i}\kappa\hat{x}) = \text{c.c.} = 0. \tag{2.13}$$

The constants p and r only depend on the velocity ratio R, and their behaviour in the limit $R \to 0$ is worth noting here: the inverse group velocity p approaches unity and r has the expansion $r = -0.9648 - 0.063\mathrm{i}R - 0.48R^2 + O(R^3)$. As has to be expected from the extension of Gaster's transformation discussed in Monkewitz & Huerre (1982), r assumes at $R = 0$ the value already found by Kelly (1967) in the temporal case (his quantity μ for case (3) of his table 1). The values for p and r are compiled in table 1 for different values of R. Also included in the table is a quantity q/R which will be introduced in §4 in connection with the modelling of non-parallel effects and a critical α_c to be discussed in the next section. At this point, the quality of the expansion of the subharmonic around $\omega^{(\beta)} = \frac{1}{2}$ can be assessed on figure 4, where the exact dispersion relation $k(\omega)$ is compared to the linearized relation $k(\omega) \approx k(\frac{1}{2})+p(\omega-\frac{1}{2})$. Fortunately, $\omega = \frac{1}{2}$ lies to the right of the most amplified frequency, so that increasing non-dimensional frequency (e.g. a growing mixing layer) leads to a decrease of the linearized growth rate. The associated neutral frequency is, however, too high (1.28 at $R = 1$ and 2.86 at $R = 0.1$ as opposed to 1).

To solve the amplitude equation (2.13), using the result (2.9) for $A(\hat{x},\hat{t})$ with $A_0 = 1$, the frequency of the subharmonic is taken to be $\omega^{(\beta)} = \frac{1}{2}+\alpha(\frac{1}{2}\Omega^{(\alpha)}+\Omega^{(\beta)})$, thus

R	p	q/R	r	$\alpha_c \times 10^2$
1.0	(1.3332+0.2768i)	(0.3539−0.1392i)	(−1.8024−0.2447i)	1.507
0.8	(1.1965+0.1366i)	(0.2897−0.1058i)	(−1.3890−0.1118i)	0.978
0.6	(1.1016+0.0720i)	(0.2565−0.0739i)	(−1.1678−0.0576i)	0.552
0.4	(1.0425+0.0378i)	(0.2386−0.0467i)	(−1.0461−0.0302i)	0.245
0.2	(1.0102+0.0165i)	(0.2296−0.0226i)	(−0.9840−0.0132i)	0.061
0.1	(1.0025+0.0080i)	(0.2275−0.0112i)	(−0.9696−0.0064i)	0.015

TABLE 1. The coefficients of (2.13) and (4.5), and the critical fundamental amplitude α_c as a function of the velocity ratio R

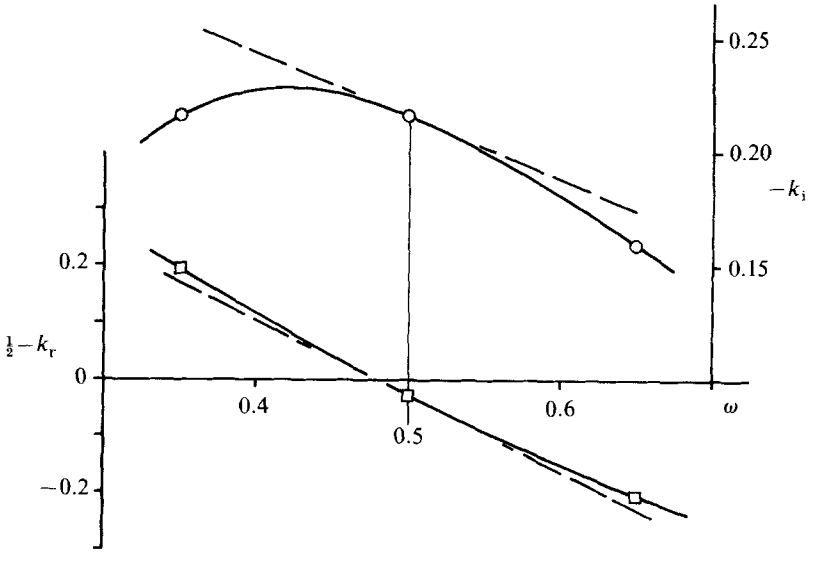

FIGURE 4. Spatial eigenvalue $k_r + ik_i$ versus frequency for $R = 1$ (——) with linearization around $\omega = 0.5$ (– –). ○, $-k_i$; □, $\frac{1}{2}-k_r$.

allowing a small deviation $\alpha\Omega^{(\beta)}$ from the exact 1:2 relationship between subharmonic and fundamental. This leads to the following structure of the solution:

$$B(\hat{x},\hat{t}) = \exp[\tfrac{1}{2}\mathrm{i}\Omega^{(\alpha)}(p\hat{x}-\hat{t})]\{B^{+}(\hat{x})\exp[\mathrm{i}\Omega^{(\beta)}(p\hat{x}-\hat{t})]+B^{-}(\hat{x})\exp[-\mathrm{i}\Omega^{(\beta)}(p\hat{x}-\hat{t})]\}. \tag{2.14}$$

Insertion into (2.13) yields four ordinary differential equations for $B^{\pm}$ and $B^{\pm}{}^{*}$,

$$B^{\pm}_{\hat{x}} + rB^{\mp}{}^{*}\exp\left\{\mathrm{i}\hat{x}\left[2\kappa+\Omega^{(\alpha)}\left(\frac{\pi}{\pi-2\mathrm{i}R}-p_r\right)\mp 2\mathrm{i}p_i\Omega^{(\beta)}\right]\right\} = \text{c.c.} = 0. \tag{2.15}$$

From this, two second-order equations for $B^{\pm}$ can be derived. The boundary conditions though, imposed, say, at $\hat{x} = 0$ in terms of real amplitudes $B_0^{\pm}$ and phases

$\frac{1}{2}\theta^{\pm}$, have to be derived from the original first-order equations (2.15), as $B^{\pm}(0)$ and $B^{\pm}_{\hat{x}}(0)$ cannot be prescribed independently. We then have

$$B^{\pm}_{\hat{x}\hat{x}} + B^{\pm}_{\hat{x}}\left\{-\mathrm{i}\left[2\kappa + \Omega^{(\alpha)}\left(\frac{\pi}{\pi - 2\mathrm{i}R} - p_{\mathrm{r}}\right)\right] \mp 2p_{\mathrm{i}}\,\Omega^{(\beta)}\right\} - |r|^2 B^{\pm} \exp\left\{-\frac{4R\pi}{\pi^2 + 4R^2}\Omega^{(\alpha)}\hat{x}\right\} = 0, \quad (2.16)$$

$$B^{\pm}(0) = B_0^{\pm} \exp\left(\tfrac{1}{2}\mathrm{i}\theta^{\pm}\right), \quad B^{\pm}_{\hat{x}}(0) = -rB^{\mp *}(0). \quad (2.17)$$

Before proceeding to the next section it is worth noting that the above equations have closed-form solutions in terms of modified Bessel functions: in simplifying the notation, the equation

$$f_{\hat{x}\hat{x}} - c_1 f_{\hat{x}} - c_0^2 f \exp(\gamma\hat{x}) = 0 \quad (2.18)$$

has the general solution

$$f = \exp\left(\tfrac{1}{2}c_1\hat{x}\right)\left\{C_I I_{c_1/\gamma}\left[\frac{2c_0}{\gamma}\exp\left(\tfrac{1}{2}\gamma\hat{x}\right)\right] + C_K K_{c_1/\gamma}\left[\frac{2c_0}{\gamma}\exp\left(\tfrac{1}{2}\gamma\hat{x}\right)\right]\right\}. \quad (2.19)$$

The order of the modified Bessel functions I and K is in general complex, which makes the evaluation of such a solution unattractive. Instead, a simple fourth-order Runge–Kutta scheme is employed for all examples following in the next sections.

3. Results for a parallel mixing layer

3.1. *The critical fundamental amplitude*

First the very simplest case is addressed, where the frequency deviations $\Omega^{(\alpha)}$ and $\Omega^{(\beta)}$ in (2.14) are zero. In other words, one is dealing with an exactly neutral fundamental and its exact subharmonic. For this situation the two amplitudes $B^{\pm}$ are identical and are merged into one quantity B. The equation (2.16) then becomes of the constant coefficient type,

$$\left.\begin{aligned} B_{\hat{x}\hat{x}} - 2\mathrm{i}\kappa B_{\hat{x}} - |r|^2 B &= 0, \\ B(0) &= B_0 \exp\left(\tfrac{1}{2}\mathrm{i}\theta\right), \\ B_{\hat{x}}(0) &= -rB^*(0), \end{aligned}\right\} \quad (3.1)$$

and is readily solved to yield

$$\left.\begin{aligned} B(\hat{x}) = B_0\,\mathrm{e}^{\mathrm{i}\kappa\hat{x}}\left\{\mathrm{e}^{\frac{1}{2}\mathrm{i}\theta}\cosh\sigma\hat{x} - \sinh\sigma\hat{x}\left[\mathrm{i}\frac{\kappa}{\sigma}\mathrm{e}^{\frac{1}{2}\mathrm{i}\theta} + \frac{r}{\sigma}\mathrm{e}^{-\frac{1}{2}\mathrm{i}\theta}\right]\right\}, \quad |\kappa| \neq |r| \\ \sigma \equiv [|r|^2 - \kappa^2]^{\frac{1}{2}}, \end{aligned}\right\} \quad (3.2a)$$

$$B(\hat{x}) = B_0\,\mathrm{e}^{-\mathrm{i}|r|\hat{x}}\{\mathrm{e}^{\frac{1}{2}\mathrm{i}\theta} + \hat{x}[\mathrm{i}|r|\,\mathrm{e}^{\frac{1}{2}\mathrm{i}\theta} - r\mathrm{e}^{-\frac{1}{2}\mathrm{i}\theta}]\}, \quad \kappa = -|r|. \quad (3.2b)$$

At critical conditions $\kappa_{\mathrm{c}} = -|r|$, the solution (3.2$a$) changes from oscillatory to exponential behaviour via the linear behaviour (3.2b). This transition lends itself directly to physical interpretation. Using the definition (2.12) of the detuning parameter, the critical κ_{c} translates into a critical fundamental amplitude

$$\alpha_{\mathrm{c}} = |\tfrac{1}{2} - k_{\mathrm{r}}|\,|r|^{-1}, \quad (3.3)$$

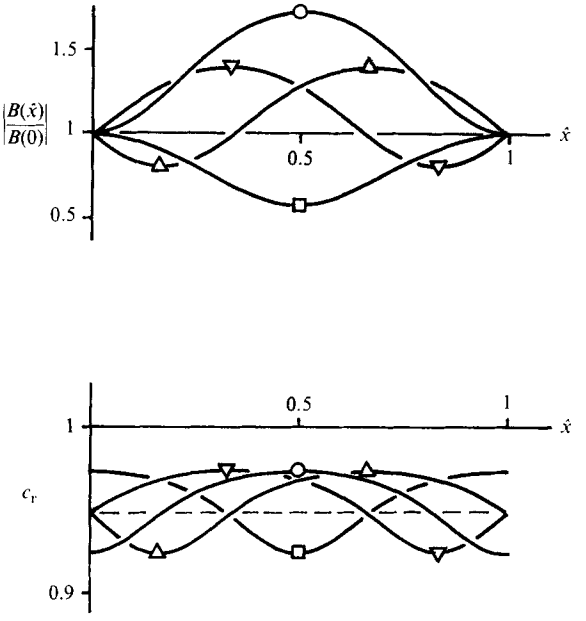

FIGURE 5. Evolution of the subharmonic amplitude for $\alpha = \frac{1}{2}\alpha_c$ and different initial phase angles $(\rho-\theta)$; △, 0; □, $\frac{1}{2}\pi$; ▽, π; ○, $\frac{3}{2}\pi$ [$R = 1$, $\rho = 1.043\pi$, $\Omega^{(\alpha)} = \Omega^{(\beta)} = 0$].

which is also listed in table 1 for different values of R. An excellent fit for α_c is given by $\alpha_c \approx 0.0153R^2$. It is noted here that for perfect tuning, which is achieved in the temporal case, the critical amplitude is zero.

For an amplitude α below critical, the amplitude function B which multiplies the exponential growth factor of the subharmonic is oscillatory, as illustrated by figure 5. The parameter varied in this figure is the initial relative phase angle θ in (3.1), which has been combined with the phase angle of the constant $r = |r| \exp(i\rho)$ for convenience. Also included in the figure is the total real phase velocity of the subharmonic, which is calculated as follows: after reconverting all slow scales into fast ones, the subharmonic has the general form

$$f(x,t) = |f(x,t)| \exp[ig(x,t)]$$

with g real. The phase velocity is then given by $c_r = g_t/g_x$. Practically, g_t and g_x are best computed by using $g_t = \omega^{(\beta)}$ in this case and $g_x = \mathrm{Im}[f_x/f]$, where f_x is readily available either analytically in special cases or from the numerical integration of (2.16). It is seen from figure 5 that the phase velocity deviates also in an oscillatory fashion from the linear value $c_r = 0.948$ (indicated by the dashed line) in such a manner that the points of maximum amplitude B in the cycle correspond to the points where c_r is closest to 1, i.e. where the conditions for resonance are most favourable.

The next figure 6 shows the development of $|B|$ and c_r for $\alpha = \alpha_c$. The most striking difference from the previous case is that now the real phase velocity asymptotically approaches 1 like $\hat{x}^{-2}$ while the amplitude reaches the asymptotic linear growth with slope $|r|\,[2-2\sin(\rho-\theta)]^{\frac{1}{2}}$. In physical terms, the fundamental is now strong enough to produce a phase-lock with the subharmonic for optimum sustained interaction.

This leads directly to the case with $\alpha > \alpha_c$, of which an example is shown as figure 7.

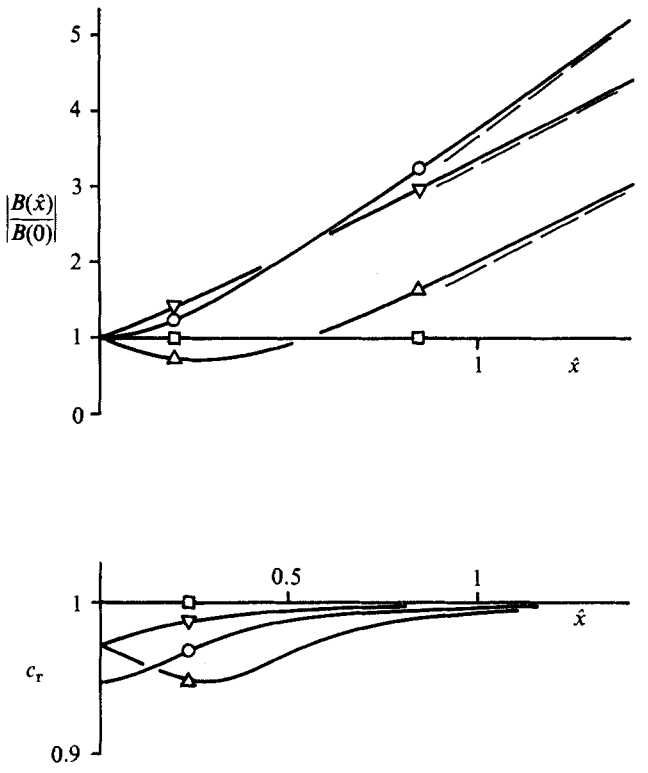

FIGURE 6. Same as figure 5, except that $\alpha = \alpha_c$.

The initial transient to produce the asymptotic optimum phase-lock by locally speeding up or slowing down the subharmonic is more violent, as c_r now approaches 1 exponentially. Also very obvious is the fact that, although the initial slope

$$\left.\begin{aligned} |B|_{\hat{x}}(\hat{x}=0) &= -2|r|\cos(\rho-\theta), \\ r &\equiv |r|\exp(\mathrm{i}\rho) \end{aligned}\right\} \quad \text{with} \tag{3.4}$$

depends trigonometrically on the phase angle θ, all but one angle lead, after a transient, to the same asymptotic exponential growth proportional to $\exp(+\sigma x)$ (cf. (3.2*a*)) which comes on top of the linear growth. The only angle which, in this simple case, produces a sustained exponential decay of B is given by

$$(\rho-\theta)_{\text{decay}} = \tan^{-1}[\alpha_c(\alpha^2-\alpha_c^2)^{-\frac{1}{2}}], \tag{3.5}$$

which is 0.064π for $\alpha = 5\alpha_c$ on figure 7. This pure decay is only possible for a truly parallel flow and $\Omega^{(\alpha)} = \Omega^{(\beta)} = 0$, and is unstable with respect to an infinitesimal disturbance of the initial angle given by (3.5). Therefore it will not be encountered in nature. Furthermore it is noted that most angles only lead to minor amplitude transients and to a $B(\hat{x})$ substantially similar to the one produced by the optimum θ.

Associating enhanced subharmonic growth with what is commonly called 'pairing' and 'shredding' with large 'dips' in $|B|$, i.e. with a reduction of total growth rate over a substantial streamwise interval, this explains why in experiments the *pairing* interaction is so heavily favoured. The bias is in fact so strong that, to the author's

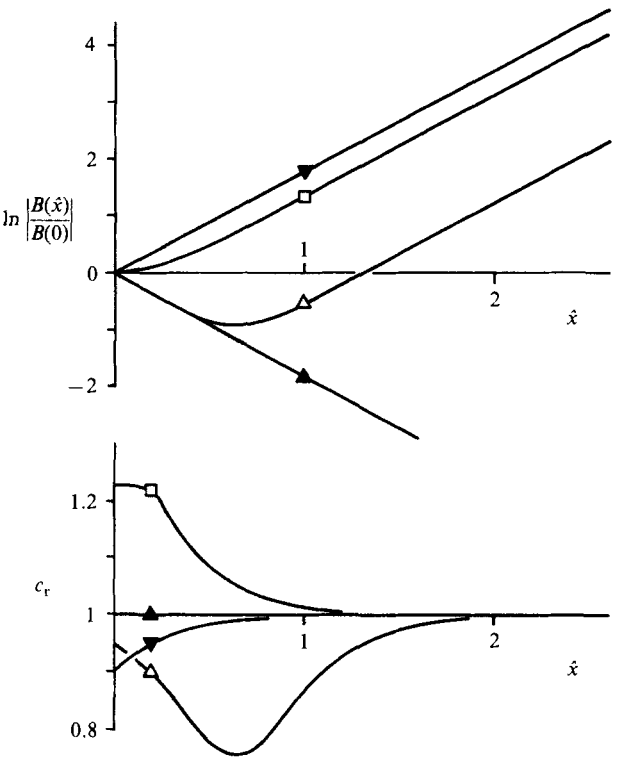

FIGURE 7. Evolution of the subharmonic amplitude for $\alpha = 5\alpha_c$ and different initial phase angles $(\rho - \theta)$: △, 0; ▲, 0.064π; □, $\frac{1}{2}\pi$; ▼, 1.064π [$R = 1$, $\rho = 1.043\pi$, $\Omega^{(\alpha)} = \Omega^{(\beta)} = 0$].

knowledge, it has been impossible to map out (by conditional-sampling techniques) the vorticity field during *shredding*. The occasional occurrence of *shredding* has only been inferred from flow visualization or indirect measurements.

At this point it is also instructive to investigate the asymptotic phase relation between fundamental and subharmonic after the phase-lock is established and B grows exponentially. First it is noted that this ultimate phase relation is the same for any initial angle θ except for the one given by (3.5). To facilitate its physical interpretation, the vorticity extrema of the fundamental and the subharmonic are examined. Their relative position is indicated on figure 8(*a*) for all the cases of ultimate exponential growth and 8(*b*) for the case of exponential decay characterized by (3.5). Positive vorticity is thereby defined as being of the same sign as the mean vorticity. It is seen from this figure that the arrangement (*a*) is precisely the one which leads to *pairing* in the numerical work of Patnaik *et al.* (1976), with the 'core' of the subharmonic midway between the cores of the short wave. The 'core' of the subharmonic, following their terminology, is located approximately midway between its two local maxima which have been connected for clarity on figure 8 (cf. their figure 13). Correspondingly, the case (*b*) leads to *shredding*. If the maxima in figure 8 are viewed as concentrated vortices, the difference between (*a*) and (*b*) can also be understood in terms of vortex interactions: while in (*a*) the subharmonic 'vortices' displace the fundamental 'vortices' (solid symbols), thus creating more subharmonic, their influence on the fundamental in (*b*) approximately cancels.

One may ask now whether the concept of critical fundamental amplitude has any

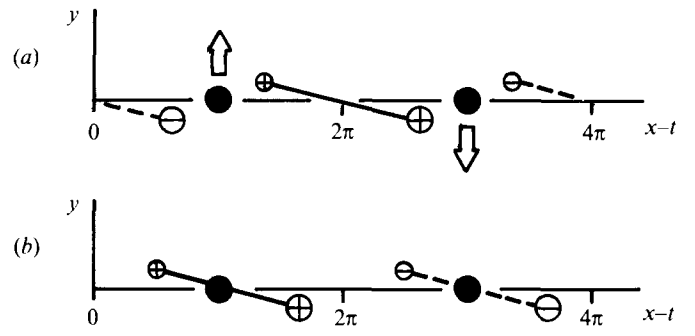

FIGURE 8. The asymptotic phase-locked arrangement of the subharmonic vorticity maxima (⊕, clockwise) and minima (⊖) relative to the fundamental maxima (●, clockwise) for (*a*) $\rho-\theta \neq 0.064\pi$, and (*b*) $\rho-\theta = 0.064\pi$. The other parameters are as in figure 7. The resulting displacement of the fundamental 'vortices' is indicated by arrows.

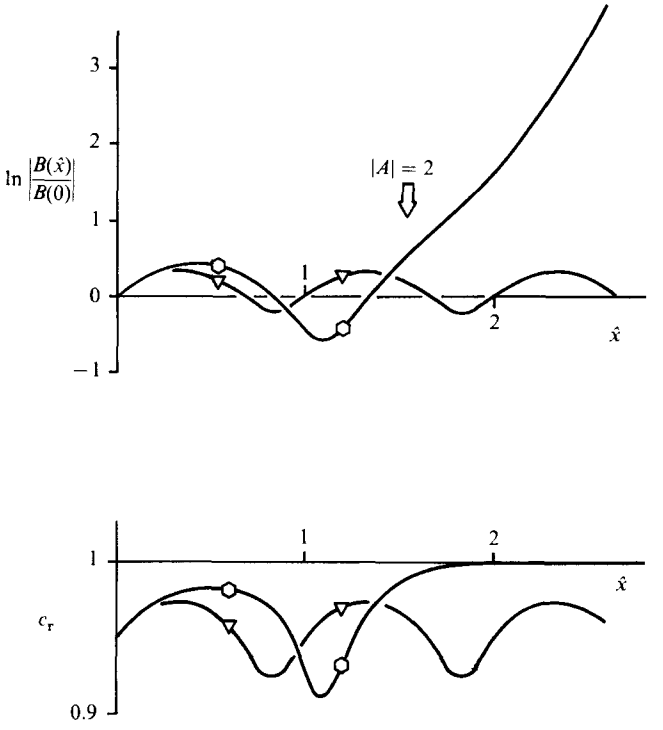

FIGURE 9. The evolution of the subharmonic amplitude (⬡) under the influence of a growing fundamental with $\Omega^{(\alpha)} = -1$, starting at a subcritical amplitude $\alpha = \frac{1}{2}\alpha_c$ [$R = 1$, $\Omega^{(\beta)} = 0$, $\rho-\theta = \pi$]. The location where the fundamental reaches critical amplitude is indicated by an arrow. ▽, reference case with neutral fundamental and same initial conditions.

merit in cases other than the very special one considered above. To answer this question (positively) two situations are considered: one with an amplified fundamental starting at half the critical amplitude, and a second with a damped fundamental starting at twice the critical amplitude. The fundamental amplitude thus crosses critical from below and above respectively, and the results shown on figures 9 and 10 clearly demonstrate that at these locations the behaviour of B changes from oscillatory to (double) exponential growth and vice versa.

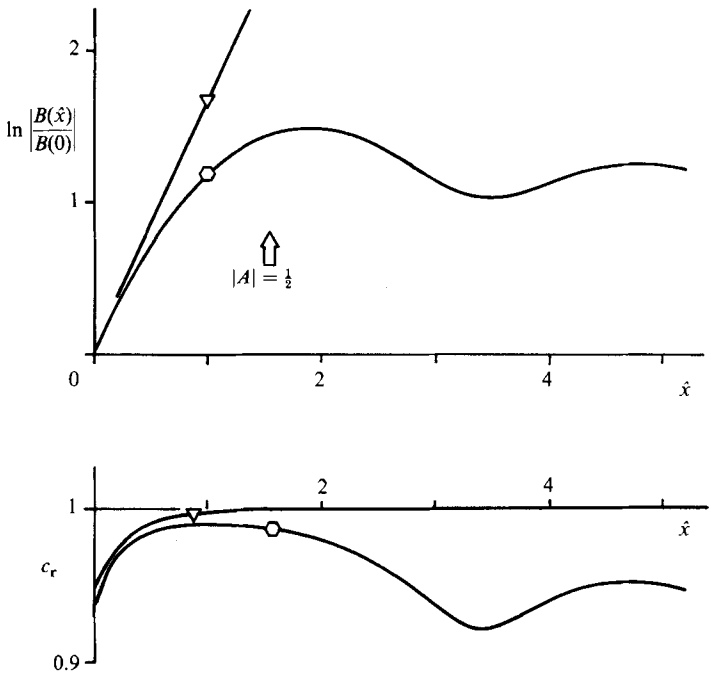

FIGURE 10. The evolution of the subharmonic amplitude (○) under the influence of a damped fundamental with $\Omega^{(\alpha)} = +1$, starting at a supercritical amplitude $\alpha = 2\alpha_c$. Otherwise as in figure 9.

Next, numerical and experimental evidence for the above findings is considered. First, the effect of phase on the interaction is amply documented in numerical studies by Patnaik *et al.* (1976), Riley & Metcalfe (1980) and others. What is not documented in these simulations are the initial transients most prominent on figure 7. They were found in a related calculation by Collins (1982), reproduced here as figure 11. It has to be pointed out, though, that this example deals with a stratified Holmboe flow where, owing to the added dimension of Richardson number, more resonances are possible; in particular, figure 11 shows the amplitude of a temporally amplifying fundamental interacting with a neutral subharmonic, the opposite of the situation considered in this paper. Nevertheless, the qualitative correspondence is encouraging, as the interaction considered by Collins could be treated along the same lines as the present problem. More recently, Arbey & Ffowcs Williams (1984) have reported on experiments in which both fundamental and subharmonic were excited in a circular jet at a relatively high level. For the case where the subharmonic was excited at a lower level than the fundamental, they found a strong dependence of the subharmonic amplitude on the relative phase and a substantially weaker effect on the fundamental. This appears to support the present analysis, although other explanations cannot be excluded at such high forcing levels. It is only very recently that Husain & Hussain (1986) have experimentally documented the effect of initial phase angle, including the initial transient behaviour, in sufficient detail to allow a generally very favourable comparison with the present results.

Secondly, evidence is examined for the critical-amplitude behaviour, which is an effect strictly associated with spatial evolution. No support has been found in numerical work, for lack of spectral information. The strongest direct evidence for

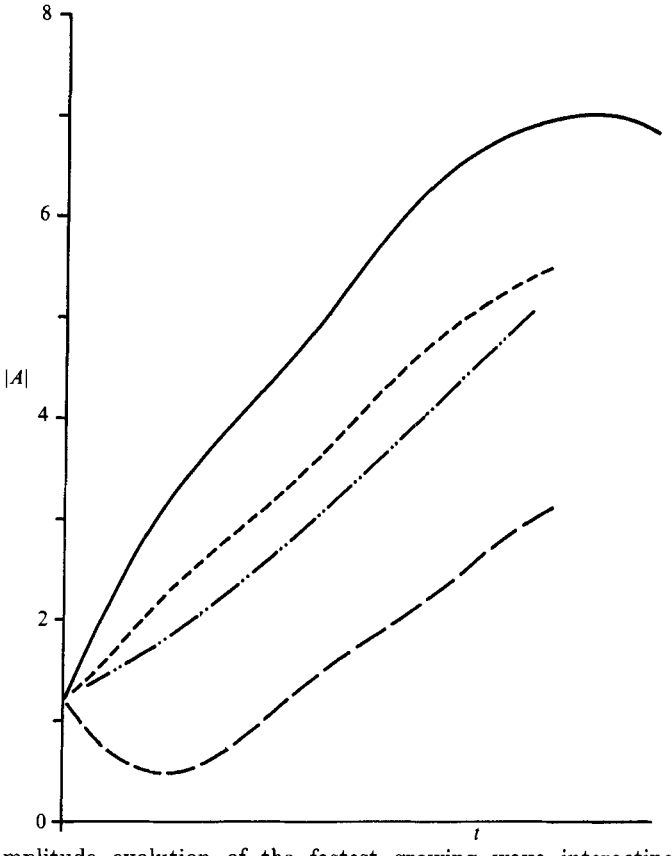

FIGURE 11. Amplitude evolution of the fastest growing wave interacting with its neutral subharmonic as a function of their relative phase φ for (stratified) Holmboe flow after Collins (1982). ——, $\varphi = 0$; ------, $\frac{1}{2}\pi$; – –, π; – · –, fastest growing wave alone (Reynolds number = 200, Prandtl number = 0.72, Richardson number = 0.174, wavenumber $k = 0.45$).

this behaviour has been obtained from the extremely clean jet-flow study of Drubka (1981). An example of his results is reproduced as figure 12 (Drubka's figure 75). It very clearly shows three stages of the subharmonic growth. First there is the initial exponential growth. Then, at approximately $x/D = 0.1$, oscillations around this exponential growth set in, leading at $x/D = 0.33$ to a distinct break in the growth rate, which assumes a higher value until the fundamental starts decaying. This behaviour bears a striking qualitative resemblance to figure 9, which encourages a quantative check: in all the cases with clean potential flow (Drubka's case 1L) the values of the fundamental amplitude α_c have been estimated at the points where the growth rate changes abruptly. As the measurements are only reported on a ray of constant mean velocity, these estimates, gathered in table 2, are rather inaccurate. However, both the oscillatory behaviour and the break in growth rates have been fully confirmed by more complete measurements involving cross-stream traverses (H. Nagib, private communication). Although the theoretical assumption of a neutral fundamental is considerably strained at these low values of α, the estimated α_c are found to be of the same order as the theoretical value of 0.015 predicted for $R = 1$. In addition, the growth-rate modification due to the presence of the fundamental with amplitude $\alpha = 0.06$ and saturation amplitude $\alpha = 0.15$ is indicated of figure 12 and compares favourably with the data.

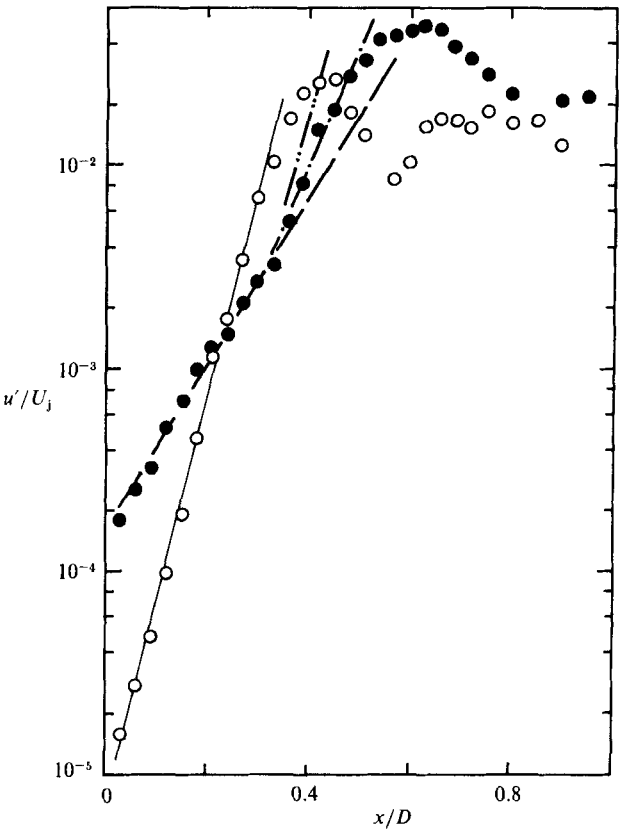

FIGURE 12. Development of the initial axisymmetric mode (○) and its subharmonic (●) along the ray $U/U_j = 0.6$ in a circular jet with $Re_D = 42000$ after Drubka (1981). ––, linear subharmonic growth; –·–, growth-rate modification for $\alpha = 0.06$; –· · –, growth-rate modification for $\alpha = 0.15$.

$Re_D \times 10^{-4}$	$\alpha_c^{(exp)}$
3.4	0.018 (+20%)
4.2	0.016 (+ 7%)
5.2	0.008 (−47%)
8.0	0.007 (−53%)

TABLE 2. Critical amplitudes $\alpha_c^{(exp)}$ estimated from Drubka's (1981) jet flow study, with percentage deviation from the theoretical prediction $\alpha_c = 0.015$. Cases are identified by Reynolds numbers.

3.2. *The excitation of a sideband of the subharmonic, and amplitude modulation*

Another feature of subharmonic resonance which is not easily accessible to numerical simulations using periodic boundary conditions in the streamwise direction, is the amplitude modulation resulting from the excitation of a sideband of the subharmonic, i.e. of a pair of modes with a frequency ratio slightly deviating from 2:1. To simplify matters, the fundamental is chosen to be exactly neutral, i.e. $\omega^{(\alpha)} = 1$, and the subharmonic is forced at $\omega^{(\beta)} = \frac{1}{2} + \alpha\Omega^{(\beta)}$. From (2.14) it is clear that the symmetric sideband at $\omega = \frac{1}{2} - \alpha\Omega^{(\beta)}$ will also emerge, resulting in a strong

amplitude modulation of the subharmonic for sidebands sufficiently close to $\omega = \frac{1}{2}$. With the simplified boundary condition where only one sideband is excited,

$$\left.\begin{aligned} B^+(0) &= B_0 e^{\frac{1}{2}i\theta}, \quad B^+_{\hat{x}}(0) = 0, \\ B^-(0) &= 0, \quad B^-_{\hat{x}}(0) = -rB^{+*}(0), \end{aligned}\right\} \tag{3.6}$$

and with $\Omega^{(\alpha)} = 0$ and $r = |r| \exp(i\rho)$, the solution of (2.16) is found to be

$$\left.\begin{aligned} B^+ &= \frac{B_0}{\mu^+ - \mu^-} e^{\frac{1}{2}i\theta}\{-\mu^- e^{\mu^+\hat{x}} + \mu^+ e^{\mu^-\hat{x}}\}, \\ \mu^\pm &= \pm[|r|^2 + (i\kappa + p_i\Omega^{(\beta)})^2]^{\frac{1}{2}} + i\kappa + p_i\Omega^{(\beta)}, \\ B^- &= -\frac{B_0}{\nu^+ - \nu^-}|r| e^{i(\rho - \frac{1}{2}\theta)}\{e^{\nu^+\hat{x}} - e^{\nu^-\hat{x}}\}, \\ \nu^\pm &= \pm[|r|^2 + (i\kappa - p_i\Omega^{(\beta)})^2]^{\frac{1}{2}} + i\kappa - p_i\Omega^{(\beta)}. \end{aligned}\right\} \tag{3.7}$$

To show the structure of the above solution more clearly, an approximation for small $\Omega^{(\beta)}$ is developed. It turns out that the following combination ϵ is the appropriate expansion parameter:

$$\epsilon \equiv \Omega^{(\beta)} p_i |r|^{-1} \ll 1. \tag{3.8}$$

Introducing the notation $n = \alpha_c/\alpha$, the detuning parameter κ, defined by (2.12), can be written as $\kappa = -|r|n$. With this, the result (3.7) is expanded up to linear order in ϵ. Furthermore, attention is concentrated on the asymptotic region of exponential growth of $B^\pm$, where the terms proportional to $\exp(\mu^-\hat{x})$ and $\exp(\nu^-\hat{x})$ are negligible and can be discarded. After a fair amount of straightforward algebra one finds for the stream function $\psi^{(\beta)}$, using (2.7) and (2.14),

$$\begin{aligned} \psi^{(\beta)} = \frac{B_0}{N}\phi(y) \exp[\tfrac{1}{2}i(x - t + \varphi_1) - k_i x + |r| N\hat{x}] \\ \times\{\cos[\Omega^{(\beta)}(C^{-1}\hat{x} - \hat{t}) - \varphi_2] - \frac{\epsilon}{2N}\exp[i\Omega^{(\beta)}(C^{-1}\hat{x} - \hat{t}) - i\varphi_2] + O(\epsilon^2)\}, \end{aligned} \tag{3.9}$$

where

$$\varphi_1 = \rho + \pi + \tan^{-1}\left(\frac{n}{N}\right),$$

$$2\varphi_2 = \rho - \theta + \pi - \tan^{-1}\left(\frac{n}{N}\right) - \epsilon n N^{-2},$$

$$C^{-1} = p_r - \epsilon\frac{n|r|}{N\Omega^{(\beta)}} \equiv p_r - \frac{p_i n}{N},$$

$$n \equiv \frac{\alpha_c}{\alpha} < 1,$$

$$N \equiv [1 - n^2]^{\frac{1}{2}} = O(1).$$

This approximate form of the solution is now amenable to discussion. It is seen from the example shown as figure 13 that the two amplitude functions B^+ and B^- very quickly reach a comparable magnitude, but that the real phase speed of either sideband does not approach 1 as before. What happens is that the two sidebands combine to an *amplitude modulated subharmonic where the carrier has a phase speed of*

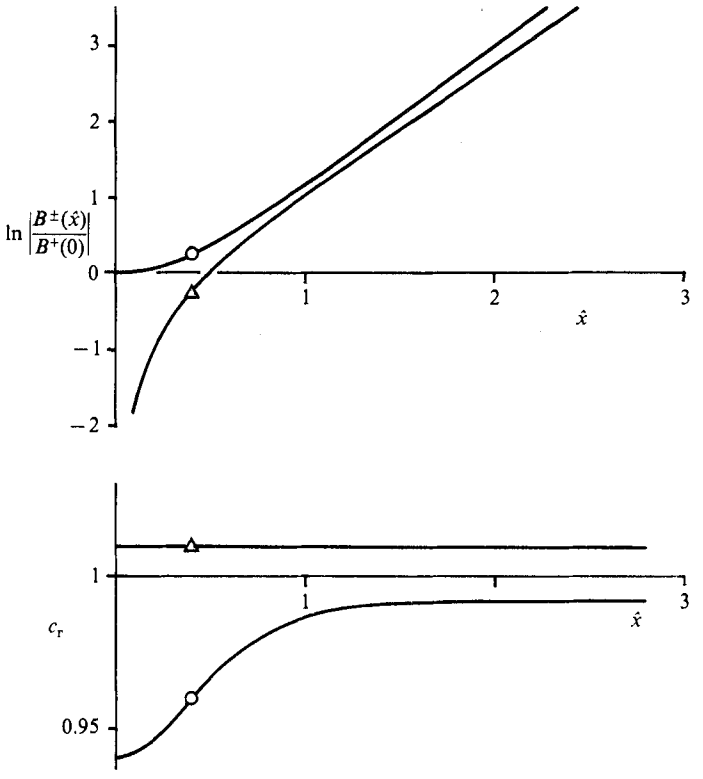

FIGURE 13. Amplitude evolution of the two sideband amplitudes B^+ (○) and B^- (△) with excitation of B^+ alone. [$R = 1$, $\Omega^{(\alpha)} = 0$, $\Omega^{(\beta)} = 0.2$, $\alpha = 5\alpha_c$, $\rho - \theta = \pi$].

unity for optimum interaction, while the modulation moves at a different speed C given by (3.9) which depends on $n = \alpha_c/\alpha$. In the limit $n \to 1$ the above expansion (3.9) is obviously not valid since $N \to 0$. As α increases beyond α_c the modulation phase speed C first goes through an unphysical singularity near $n \approx 1$, then decreases and, for $R = 1$, crosses $C = 1$ at $n = 0.77$. For large amplitudes (i.e. $n \to 0$), C then approaches from above the asymptote p_r^{-1} which is well approximated by $C(n = 0) \approx 1 - 0.25R^2$ (cf. table 1). Furthermore, as long as the condition (3.8) is satisfied, the modulation is almost total, i.e. the ratio of minimum to maximum amplitude is $\epsilon/2N \ll 1$.

When looking for evidence of amplitude modulation (AM) in the mixing layer, one finds that modulation is ubiquitous except in experiments with controlled forcing. Monkewitz (1983) has investigated the AM of the initial disturbance in a circular jet where it appears to be generated at the nozzle lip. This is a special case, though, since the initial disturbance is the only shear-layer mode that is not the subharmonic of a mode peaking further upstream. Therefore the mechanism of AM generation considered here cannot apply to the initial disturbance. The modulation, however, is still present after many pairings, as shown by Browand (1966) and others (cf. Browand's hot-wire traces). Furthermore, beyond the initial disturbance, the modulation frequency appears to scale with the local 'carrier' passage frequency $\omega^{(\beta)}$ and is of the order of $0.1\omega^{(\beta)}$. It is in this region that an explanation for the pervasive amplitude modulation of instability waves in mixing layers is proposed.

The comparison of the result (3.7) or (3.9) with measurements rests on the choice of $\Omega^{(\beta)}$. To pick a particular frequency detuning $\Omega^{(\beta)}$, one may argue that in the early stages, given a reasonably broadband forcing (controlled or uncontrolled), the linearly most amplified mode at $\omega^{(\max)}$ is likely to compete with the mode at $\omega = \frac{1}{2}$. It is therefore reasonable to choose as a typical detuning $|\alpha\Omega^{(\beta)}| = |\omega^{(\max)} - \frac{1}{2}|$ which is approximately equal to 0.08 at $R = 1$. Some support for this choice is obtained from figures 12 and 13 of Laufer & Zhang (1983) where, despite the forcing, two sidebands of the first subharmonic f_1 are clearly visible and separated quite accurately by $\pm 0.08 f_0$ from the main peak. Further downstream where the second subharmonic grows fastest (their figures 14–17) there is only a scant indication of sidebands but the peak f_2 is much broader and in fact has a width of approximately $0.15 f_1$, thus including the two typical sidebands.

From this, the following picture emerges for the spectral evolution of a subharmonic under natural excitation: Initially, the spectrum contains a wide range of frequencies around the subharmonic, i.e. noise, with a small peak at the exact subharmonic which is possibly due to a weak feedback mechanism as postulated by Laufer & Monkewitz (1980). First, this spectrum develops according to linear theory with, in addition to the exact subharmonic peak, a broad peak forming around $\omega^{(\max)}$. Then the subharmonic waves enter a region where the fundamental has an amplitude sufficiently larger than critical. There, the resonant interaction boosts the range of frequencies where it is most effective and produces the final pronounced spectral peak. From the above discussion and from the inspection of $(\frac{1}{2} - k_r)$ on figure 4, this range of effectiveness or minimal detuning appears well characterized by $|\omega^{(\max)} - \frac{1}{2}|$. In addition to significantly boosting the frequencies close to the subharmonic, the resonance does also '*symmetrize*' the spectral peak with respect to exactly half of the fundamental frequency no matter how skewed the peak is before the resonance. This is achieved by the production of symmetric sidebands, as shown by the example of this section (figure 13). This plausible scenario is capable of providing an explanation for features of the mixing layer that have so far eluded theoretical interpretation, such as the widely observed amplitude modulation of instability waves as well as the width and symmetry of the subharmonic spectral peak under 'natural', i.e. low-level and broadband excitation. A test of this proposed sequence of events, however, is lacking except for some very recent experiments by Husain & Hussain (1986) who systematically excited sidebands of the subharmonic and found encouraging support for this aspect of the suggested scenario.

3.3. *The case of slightly oblique subharmonic waves*

So far only the purely two-dimensional case has been considered. However, the real mixing layer has a distinct spanwise structure. Apart from a 'streakiness' on a small scale which will not be addressed here, the large-scale structures are known to have a large but finite 'aspect ratio', as shown by Browand & Troutt (1980, 1985) and others. This latter observation may be modelled by considering a triad resonance between the two-dimensional fundamental and a pair of oblique subharmonics. In the planview, this results in a regular diamond pattern of subharmonic large-scale structures which can be interpreted as in the process of 'helical pairing'. The question is naturally whether a triad resonance can be found which is stronger than the two-dimensional resonance considered so far.

Formally, the following extension of the analysis is closely related to the work of Craik (1971) and more recently Smith & Stewart (1987) in the boundary layer.

However, the reader is reminded that the scope of the analysis is limited by the large subharmonic growth rate, as discussed in §2, whereas in the boundary layer growth rates approach zero in the limit of infinite Reynolds numbers. The problem is now analysed by using Squire's transformation in the inviscid form (see Drazin & Reid 1981). With it, the problem of an oblique wave, labelled 3D, with complex streamwise wavenumber k_{3D} and real transverse wavenumber γ is transformed into an equivalent two-dimensional problem, with

$$\left.\begin{aligned} k_{2D} &= [k_{3D}^2+\gamma^2]^{\frac{1}{2}}, \\ c_{2D} &= c_{3D}, \\ \omega_{2D} &= \omega_{3D}[1+\gamma^2 k_{3D}^{-2}]^{\frac{1}{2}}. \end{aligned}\right\} \tag{3.10}$$

For the spatial case this transformation implies complex frequency and wavenumber in the two-dimensional problem. For small transverse wavenumbers γ, the 2D and 3D cases can be approximately related as follows. Using the Taylor expansion of the dispersion relation around $\omega = \frac{1}{2}$, one has

$$\left.\begin{aligned} \omega_{2D} &= \tfrac{1}{2}+\gamma^2\Delta\omega, \\ k_{2D} &= k+\gamma^2 \frac{\mathrm{d}k}{\mathrm{d}\omega}\bigg|_{\omega=\frac{1}{2}} \Delta\omega+O(\gamma^4). \end{aligned}\right\} \tag{3.11}$$

In order to describe the evolution of the real frequency $\omega_{3D} = \frac{1}{2}-\gamma^2\Omega$, allowing for a small deviation from $\frac{1}{2}$, $\Delta\omega$ in (3.11) has to be chosen as $\Delta\omega = \frac{1}{4}(k^{-2})-\Omega$. With $\mathrm{d}k/\mathrm{d}\omega = p$ (cf. table 1), k_{3D} is then obtained as

$$\left.\begin{aligned} \omega_{3D} &= \tfrac{1}{2}-\gamma^2\Omega, \\ k_{3D} &= k+\gamma^2[p(\tfrac{1}{4}k^{-2}-\Omega)-\tfrac{1}{2}k^{-1}]+O(\gamma^4). \end{aligned}\right\} \tag{3.12}$$

For the velocity ratio $R = 1$ this yields (numerically)

$$k_{3D} = (0.5274-0.2155\mathrm{i})-\gamma^2(0.2288-0.5394\mathrm{i})-\gamma^2\Omega(1.3332+0.2768\mathrm{i}). \tag{3.13}$$

Thus the real part of k_{3D} can be made equal to $\frac{1}{2}$. For, say, $\Omega = 0$ this is achieved with a transverse wavenumber $\gamma = 0.35$. Hence the associated detuning parameter κ (cf. (2.12)) is zero and the resonance is enhanced. The growth rate $-k_{\mathrm{i},3D}$, on the other hand, is decreased at the same time from 0.2155 to 0.151. Such a three-dimensional subharmonic could therefore only grow faster than the 2D subharmonic if the difference in linear growth rates is compensated by a larger nonlinear boost. Since the nonlinear growth-rate modification is significantly affected by the detuning only for α values close to critical, it appears that the two-dimensional resonance has a slight edge over the triad resonance. The difference, however, is so small that in an experiment the selection process for γ is most likely governed by higher-order effects and/or facility characteristics. This result is entirely in agreement with the investigation of Pierrehumbert & Widnall (1982) who treated the subharmonic as a secondary instability and found its temporal growth rate to be quite insensitive to the transverse wavenumber in the range from $\gamma = 0$ to about 0.3 (cf. their figure 5, noting that their ρ equals 2α).

4. The pairing and shredding interaction and the modelling of non-parallel effects

In this section an attempt is made to analyse the essential ingredients of the so-called pairing, and of the mostly numerically observed shredding interaction. The main question here is how much of it is really due to a genuine mode interaction and how much can simply be explained by wave kinematics. To make the point, it is first demonstrated that an extremely simple kinematic model is indeed capable of reproducing what is perceived as a pairing in a typical flow-visualization experiment.

To keep matters simple, one-dimensional waves without transverse structure are chosen to represent disturbance vorticity integrated across the mixing layer. A local maximum of such a vorticity wave can therefore be directly identified with a marker (dye) concentration in a flow-visualization experiment (cf. Corcos & Sherman 1984). As 'pairing' is observed after the saturation of the short wave, the fundamental is taken to be of constant amplitude for simplicity. The subharmonic, on the other hand, is chosen to grow exponentially at the constant rate $-k_i$ and to have the same phase speed c as the fundamental. Linear superposition then yields the following expression for the vorticity disturbance:

$$\Gamma(x,t) = -\cos[x-ct] - B\,\mathrm{e}^{-k_i x}\cos[\tfrac{1}{2}(x-ct)+\varphi]. \tag{4.1}$$

If now the instantaneous local maxima of this function Γ are traced on an x–t diagram, using a set of quite realistic parameters (see figure 14), the result is startling: one recovers the typical pairing history of two vorticies as obtained from a flow-visualization movie. That is, the model correctly predicts the alternate speeding up and slowing down of vortices even though the phase speed c is taken to be a constant! This is evidenced by a comparison with unpublished visualization data of C. M. Ho (private communication) on figure 14(a, b), where c_v denotes the observed speed of the dye concentrations and the computed speed of the instantaneous local maxima of Γ respectively. It is noted, however, that the details of the pairing associated with transverse vortex displacements (see Zaman & Hussain 1980) are lost in this one-dimensional model.

In a next step one would like to incorporate the saturation of the subharmonic into a more sophisticated model of the pairing and shredding 'interaction' in order to investigate whether additional features such as transverse structure can be captured. For this purpose, following Huerre & Crighton (1983), a slightly non-parallel mean flow is introduced into the formulation of §2. As a consequence, the analysis is no longer mathematically consistent, i.e. can no longer be extended to arbitrary orders, and therefore becomes an *ad hoc* model. The reason for this is that the ordering of terms, imposed by the weakly nonlinear formulation of mode interactions, is upset by the early introduction of 'mean-flow correction' (see also the discussion in §1). An additional problem arises when, as in most studies of this type, the assumed non-parallel mean flow does not satisfy the basic equations. The reason for selecting the slightly non-parallel approach is the fact that the inconsistencies mentioned above only manifest themselves beyond the orders α^2 and $\alpha\beta$ considered in this study. On the other hand, one would have to confront these inconsistencies explicitly with a slowly diverging formulation, or with the approach of Cohen (1986), which came to the author's attention during the revision of this paper. Another approach, not considered here, is to use shape assumptions and an energy method (see for instance Liu & Nikitopoulos 1982 and Mankbadi 1985).

The essence of the slightly non-parallel approach (Huerre & Crighton 1983) is that

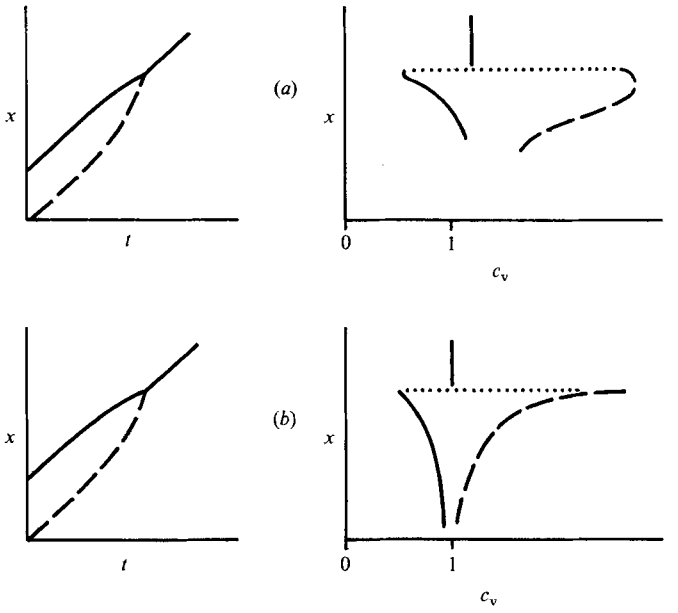

FIGURE 14. (*a*) Trajectories and velocities c_v of dye concentrations (vortices) in an organized water jet of $Re = 5000$ (from C. M. Ho, private communication). Two consecutive vortices are depicted with one slowing down (——) and the other accelerating (– –) during pairing. (*b*) Corresponding trajectories and velocities of the instantaneous local maxima of the 'vorticity wave' (4.1) with $c = 1$, $B = 1, -k_i = 0.15$ and $\varphi = 0$.

the mean-flow divergence is required to be not only slow but small as well. That is, the vorticity thickness δ_ω is now a function of the slow $\hat{x}$ (chosen to be the same as in §2) and deviates only little from $2\delta_0$, where the reference length δ_0 is conveniently identified with half the vorticity thickness at the station $\hat{x} = 0$, at which the fundamental is neutrally stable. It can therefore be written as

$$\frac{\delta_\omega(\hat{x})}{2\delta_0} = 1 + \alpha d(\hat{x}); \quad d(0) = 0. \tag{4.2}$$

Introducing this variable thickness into (2.2) and expanding in powers of α leads to

$$\bar{\psi}_y^{(0)} = 1 + R \tanh\left[y(1+\alpha d)^{-1}\right] \tag{4.3a}$$

$$\approx 1 + R \tanh y - \alpha R d(\hat{x}) y \operatorname{sech}^2 y. \tag{4.3b}$$

Expression (4.3*b*) is then integrated and introduced into (2.1) in lieu of the parallel mean flow. This leads to additional inhomogeneous terms in the equations at order α^2 and $\alpha\beta$, and hence, after applying solvability conditions, to additional terms in the amplitude equations. Without giving details of the straightforward procedure, the fundamental amplitude function A is found to be modified by the slight non-parallel effects from (2.9) to

$$\left.\begin{aligned} A(\hat{x},\hat{t}) = A_0 \exp\left\{\left[1 - \frac{2iR}{\pi}\right]^{-1}\left[i\Omega^{(\alpha)}\hat{x} - \frac{2R}{\pi}D(\hat{x})\right] - i\Omega^{(\alpha)}\hat{t}\right\}, \\ D(\hat{x}) \equiv \int d(\hat{x})\,\mathrm{d}\hat{x}, \end{aligned}\right\} \tag{4.4}$$

a result already found by Huerre & Crighton (1983) for the special case $d(\hat{x}) = \hat{x}$. Solvability at order $\alpha\beta$ leads in an analogous way to the following modification of the subharmonic amplitude equation (2.13), where q, also listed in table 1, is a new constant related to mean flow divergence:

$$B_{\hat{x}} + pB_{\hat{t}} + qd(\hat{x})B + rA(\hat{x}, \hat{t})\, B^* \exp(2i\kappa\hat{x}) = \text{c.c.} = 0. \tag{4.5}$$

The general solution of (4.5) is then finally obtained from

$$B^{\pm}_{\hat{x}\hat{x}} + B^{\pm}_{\hat{x}} \left\{ -i\left[2\kappa + \Omega^{(\alpha)}\left(\frac{\pi}{\pi - 2iR} - p_r\right)\right] \mp 2p_i\Omega^{(\beta)} + 2d(\hat{x})\left[\frac{R}{\pi - 2iR} - iq_i\right]\right\}$$
$$- |r|^2 B^{\pm} \exp\left\{-\frac{4R\pi}{\pi^2 + 4R^2}[\Omega^{(\alpha)}\hat{x} + D(\hat{x})]\right\} = 0. \tag{4.6}$$

The equation above represents the slightly non-parallel extension of (2.16). The associated boundary conditions (2.17) thereby remain unchanged.

At this point the vorticity thickness has to be specified. It has been recognized in the past that in experiments where the saturation of a mode is localized by forcing, i.e. where jitter is eliminated, the mixing layer grows in a step-like fashion (cf. Laufer & Monkewitz 1980; Ho 1982 and the experimental data of Zaman & Hussain 1980; Ho & Huang 1982). Thereby each successive step represents the mean-flow correction (in weakly nonlinear parlance) associated with essentially one mode in a subharmonic sequence. As shown on figure 24 of Ho & Huerre (1984) one can therefore isolate a 'universal step' over which the mixing-layer thickness is doubled. Guided by these experimental findings, the vorticity thickness (4.2) is now defined by superimposing a sequence of self-similar 'universal steps'. Each 'step', in turn, is given in normalized form by the function $S(\xi)$ which is somewhat arbitrarily chosen to be the integral (4.7) of sech ξ:

$$S(\xi) = \frac{1}{2} + \frac{1}{\pi}\sin^{-1}[\tanh\xi], \tag{4.7}$$

$$\left.\begin{aligned} \frac{\delta_\omega(x)}{2\delta_0} &= \left\{1 + \sum_{n=0}^{\infty} 2^n S[\xi_n(x)]\right\}\left\{1 + \sum_{n=0}^{\infty} 2^n S[\xi_n(0)]\right\}^{-1}, \\ \xi_n(x) &= 2^{-n}\lambda[x - x_0 - (2^n - 1)L]. \end{aligned}\right\} \tag{4.8}$$

In the above expression, L is the distance between 'steps'. The non-dimensional L corresponding to the experimental average spreading rate of $\bar{\delta}'_\omega \approx 0.18R$ is approximately $4\pi/R$ or $2/R$ times the fundamental wavelength. The quantity x_0 defines the location of the step relative to the saturation of the fundamental. The constant λ, finally, is chosen such that far upstream each 'mean-flow correction' S grows exponentially at twice the maximum spatial growth rate, as suggested by weakly nonlinear theory. This leads to $\lambda \approx R$, and a maximum local slope δ'_ω of twice the average.

A realization of (4.7) and (4.8), which will be used to 'produce' a pairing, is shown as figure 15 (*a*), with all the parameter values listed in the caption. The corresponding average spreading rate of $\bar{\delta}'_\omega = 0.154$ lies well within the scatter of experiments. Then, with the vorticity thickness of figure 15 (*a*), the fundamental amplitude (4.4) and the subharmonic amplitude, resulting from the integration of (4.6), are determined for zero frequency detuning $\Omega^{(\alpha)}$ and $\Omega^{(\beta)}$, and zero phase shift in the boundary conditions (2.17). As discussed in §3, this latter choice leads to an enhanced subharmonic growth, i.e. to optimal pairing. The results are plotted on figure 15 (*b*)

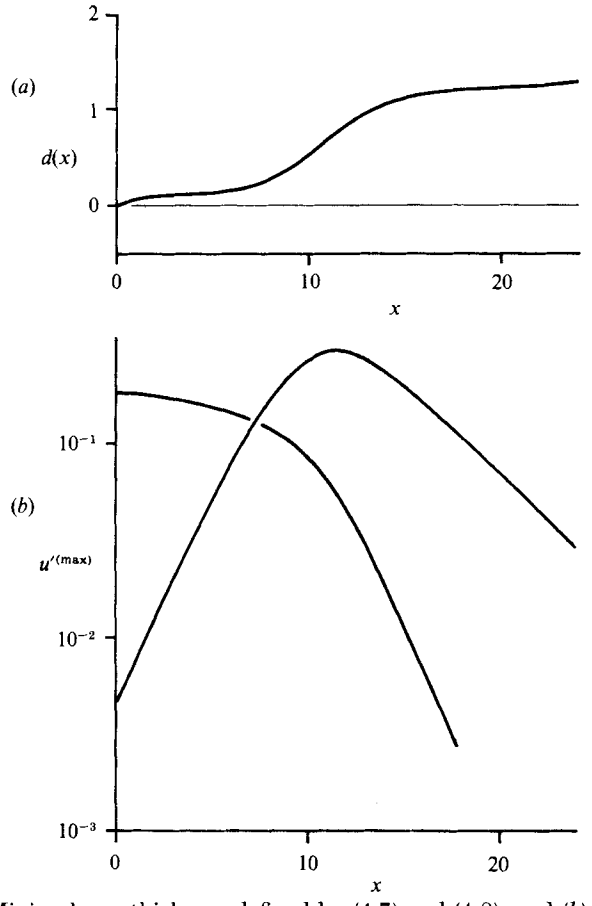

FIGURE 15. (*a*) Mixing-layer thickness defined by (4.7) and (4.8), and (*b*) corresponding maximum streamwise velocity disturbance of fundamental and subharmonic versus x for the 'pairing' of figure 16 with parameters $R = 1$, $\lambda = 1$, $x_0 = -1.25$, $L = 12$, $\alpha = 0.1875$, $\theta = 0$.

in terms of maximum streamwise velocity amplitude. Both peak amplitudes were specified as follows: $\alpha = 0.1875$, which yields a fundamental large-scale structure closest to the measurements of Browand & Weidman (1976) (cf. figure 2), and a non-dimensional (with the average velocity!) maximum subharmonic velocity disturbance $u'^{(max)} = 0.31$. This latter value was arrived at by examining the ratios of subharmonic to fundamental peak energies of Ho & Huang (1982).

The resulting total vorticity contours over two fundamental periods $T^{(\alpha)}$ are shown on figure 16. It is apparent that the early part of the pairing is described quite successfully by the present model, when compared with data of Browand & Weidman (1976) and Hussain & Zaman (1980) who also documented the early stages of pairing. It has to be noted, though, that in Browand & Weidman's case the comparisons rely on Taylor's hypothesis. The alternate speeding up and slowing down of vortices is again correctly predicted, as in the simplistic model at the beginning of this chapter. In addition, the tilting of the slowing vortices (see e.g. the 3rd frame of figure 16 where the 3rd vortex is tilted approximately 5°) before 'rolling under' is faithfully reproduced. At $t/T^{(\alpha)} = 1$ the pairing is complete, i.e. the vorticity maximum associated with the subharmonic has reached peak amplitude in the centre of the frame (cf. figure 15*b*). At this point the principal shortcoming of the slightly

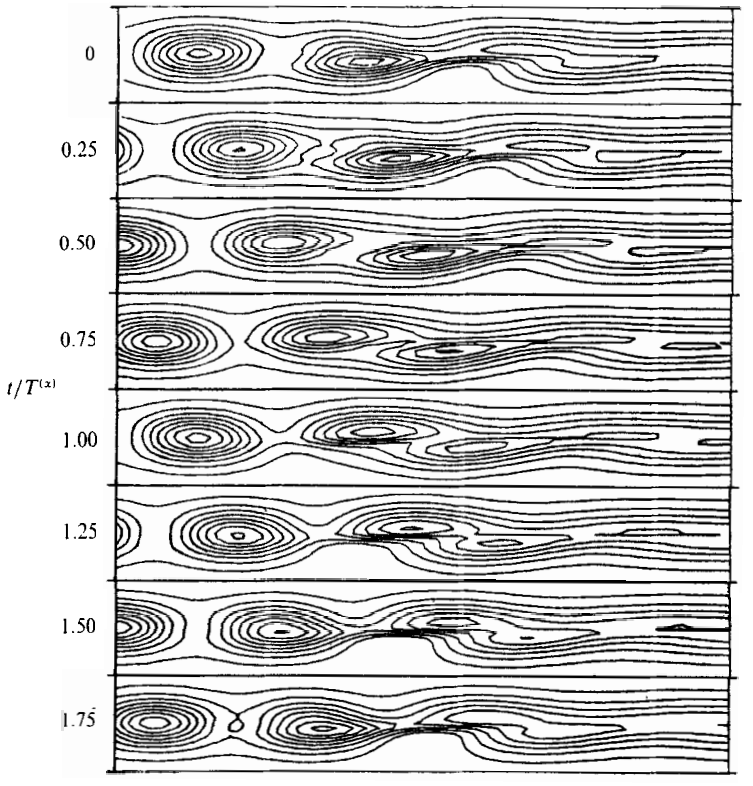

FIGURE 16. Vorticity contours for the 'pairing interaction' of figure 15 as a function of time over two fundamental periods $T^{(\alpha)}$. The size of each frame is $2\delta_\omega \times 12\delta_\omega$. The vorticity difference between contours is 0.2.

non-parallel model becomes obvious: at saturation, the subharmonic-mode shape, on a linear basis, should be sech(y), such that it can in turn assume the role of a fundamental in the next pairing sequence. In the slightly diverging formulation, however, the subharmonic-mode shape remains frozen. Therefore the subharmonic vortex on figure 16 for $t/T^{(\alpha)} > 1$ still has the two local vorticity maxima characteristic of modes close to the most amplified, which precludes the completion of the 'rolling over'. Of course, the fundamental-mode shape also remains frozen, which appears, at least optically, less annoying. In addition, the model has clearly been stretched beyond its limitations by choosing α as large as 0.1875, and by prescribing a vorticity thickness (4.8) which starts to double rapidly around $x = 8$ (figure 15*a*), i.e. beyond the first third of the frames of figure 16.

Attempts at reproducing a *shredding* interaction as computed by Patnaik *et al.* (1976) produced a rather vague resemblance to numerical results, and are not reported here. The reason is that the shortcomings of the model, noted above, become more manifest in the shredding case. This concludes the presentation of results on a somewhat disappointing note which serves to show the limitations of the slightly non-parallel model.

5. Conclusions

It has been shown that many large-scale features of the 'turbulent' mixing layer are adequately described by a (locally) parallel weakly nonlinear instability-wave analysis. In particular, the existence of a critical fundamental amplitude, required for phase locking with the subharmonic and for the modification of its growth rate, has been demonstrated and found to be in reasonable agreement with experiment. Also, the width of the subharmonic spectral peak and the subharmonic amplitude modulation, widely observed in 'natural' experiments, i.e. experiments with low-level broadband excitation, are shown to be direct consequences of the subharmonic resonance mechanism. No clear-cut conclusions, however, could be drawn regarding the preference of the mixing layer for slightly oblique or two-dimensional subharmonics since the total streamwise growth rate was found to be only weakly dependent upon the transverse wavenumber γ as long as γ was small.

In the previous section, finally, the essential ingredients for the pairing and shredding process have been investigated by considering two *ad hoc* models. One is a simple-minded kinematic wave model, and the second combines the weakly nonlinear analysis of the parallel mixing layer with the slightly non-parallel approach of Huerre & Crighton (1983). It appears from the results that the pairing in particular consists primarily of the *subharmonic 'overtaking' the fundamental without any especially strong interaction* between the two. In other words, the strongly nonlinear Biot–Savart-type vortex interaction does not seem to be the only way of explaining pairing. Along the same lines, it is thought that phenomena often related to the visually so striking 'pairing interaction', such as locally enhanced entrainment for instance, are chiefly due to the local rapid growth of the subharmonic and the associated mean flow modification, which are only relatively weakly affected by the fundamental. From the wave description it appears that the principal effect of the fundamental (its phasing), which is obviously important for the distinction between pairing and shredding, is in the latter case to delay the subharmonic growth to a region where the fundamental is already significantly decayed. The ultimate subharmonic peak amplitude, thereby, remains largely unaffected (see, for instance, Riley & Metcalfe 1980).

Lastly, the slightly non-parallel model was found to reproduce the transverse structure of fundamental and subharmonic reasonably well only in the early stages of a pairing. Beyond that point, the mode shape must be allowed to change in order to produce realistic results. As a consequence, the fundamental would have to be considered well into the damped region $\omega^{(\alpha)} \geqslant 1$, where it is advantageous to use an Orr–Sommerfeld analysis in order to obtain mode shapes.

REFERENCES

ACTON, E. 1976 The modelling of large eddies in a two-dimensional shear layer. *J. Fluid Mech.* **76**, 561–592.

ARBEY, H. & FFOWCS WILLIAMS, J. E. 1984 Active cancellation of pure tones in an excited jet. *J. Fluid Mech.* **149**, 445–454.

ASHURST, W. T. 1979 Numerical simulation of turbulent mixing layers via vortex dynamics. In *Turbulent Shear Flows I* (ed. F. Durst, B. E. Launder, F. W. Schmidt, J. H. Whitelaw), pp. 402–413. Springer.

BOUTHIER, M. 1972 Stabilité linéaire des écoulements prèsque parallèles. *J. Méc.* **4**, 599–621.

BROWAND, F. K. 1966 An experimental investigation of the instability of an incompressible, separated shear layer. *J. Fluid Mech.* **26**, 281–307.

BROWAND, F. K. & TROUTT, T. R. 1980 A note on spanwise structure in the two-dimensional mixing layer. *J. Fluid Mech.* **97**, 771–781.

BROWAND, F. K. & TROUTT, T. R. 1985 The turbulent mixing layer: geometry of large vortices. *J. Fluid Mech.* **158**, 489–509.

BROWAND, F. K. & WEIDMAN, P. D. 1976 Large scales in the developing mixing layer. *J. Fluid Mech.* **76**, 127–144.

BROWN, G. L. & ROSHKO, A. 1974 On density effects and large scale structure in turbulent mixing layers. *J. Fluid Mech.* **64**, 775–816.

CHURILOV, S. M. & SHUKHMAN, I. G. 1987 Note on weakly nonlinear stability theory of a free mixing layer. *Proc. R. Soc. Lond.* A **409**, 351–367.

COHEN, J. 1986 Instabilities in turbulent free shear flows. Ph.D. thesis, University of Arizona, Tucson.

COLLINS, D. A. 1982 A numerical study of the stability of a stratified mixing layer. Ph.D. thesis, McGill University.

CORCOS, G. M. & SHERMAN, F. S. 1984 The mixing layer: deterministic models of a turbulent flow. Part 1. Introduction and the two-dimensional flow. *J. Fluid Mech.* **139**, 29–65.

CRAIK, A. D. D. 1971 Non-linear resonant instability in boundary layers. *J. Fluid Mech.* **50**, 393–413.

CRIGHTON, D. G. & GASTER, M. 1976 Stability of slowly diverging jet flow. *J. Fluid Mech.* **77**, 397–413.

DRAZIN, P. & REID, W. 1981 *Hydrodynamic Stability.* Cambridge University Press.

DRUBKA, R. E. 1981 Instabilities in near field of turbulent jets and their dependence on initial conditions and Reynolds number. Ph.D. thesis, Illinois Institute of Technology.

GASTER, M., KIT, E. & WYGNANSKI, I. 1985 Large-scale structures in a forced turbulent mixing layer. *J. Fluid Mech.* **150**, 23–39.

GÖRTLER, H. 1942 Berechnung von Aufgaben der freien Turbulenz auf Grund eines neuen Näherungsansatzes. *Z. Angew. Math. Mech.* **22**, 244–254.

HO, C. M. 1982 Local and global dynamics of free shear layers. In *Proc. Symp. Numerical and Physical Aspects of Aerodynamic Flows* (ed. T. Cebeci), pp. 521–533. Springer.

HO, C. M. & HUANG, L. S. 1982 Subharmonics and vortex merging in mixing layers. *J. Fluid Mech.* **119**, 443–473.

HO, C. M. & HUERRE, P. 1984 Perturbed free shear layers. *Ann. Rev. Fluid Mech.* **16**, 365–424.

HUERRE, P. 1987 On the Landau constant in mixing layers. *Proc. R. Soc. Lond.* A **409**, 369–381.

HUERRE, P. & CRIGHTON, D. G. 1983 Sound generation by instability waves in a low Mach number jet. *AIAA paper* 83–0661.

HUSAIN, H. S. & HUSSAIN, A. K. M. F. 1986 Subharmonic resonance in a free shear layer. *Bull. Am. Phys. Soc.* **31**, 1696.

HUSSAIN, A. K. M. F. & ZAMAN, K. B. M. Q. 1980 Vortex pairing in a circular jet under controlled excitation. Part 2. Coherent structure dynamics. *J. Fluid Mech.* **101**, 493–544.

KÁRMÁN, T. VON & RUBACH, H. 1912 Über den Mechanismus des Flüssigkeits und Luftwiderstandes. *Phys. Z.* **13**, 49–59.

KELLY, R. E. 1967 On the stability of an inviscid shear layer which is periodic in space and time. *J. Fluid Mech.* **27**, 657–689.

LAUFER, J. & MONKEWITZ, P. A. 1980 On turbulent jet flows: a new perspective. *AIAA paper* 80–0962.

LAUFER, J. & ZHANG, X. 1983 Unsteady aspects of a low Mach number jet. *Phys. Fluids* **26**, 1740–1750.

LIU, J. T. C. & MERKINE, L. 1976 On the interaction between large scale structure and fine grained turbulence on a free shear flow. I. The development of temporal interactions in the mean. *Proc. R. Soc. Lond.* A **352**, 213–247.

LIU, J. T. C. & NIKITOPOULOS, D. 1982 Mode interactions in developing shear flows. *Bull Am. Phys. Soc.* **27**, 1192.

MANKBADI, R. R. 1985 The mechanism of mixing enhancement and suppression in a circular jet under excitation conditions. *Phys. Fluids* **28**, 2062–2074.

MANSOUR, N. N. & BARR, P. K. 1987 Simulation of turbulent mixing layers. *Proc. Fifth Symp. on Turbulent Shear Flows* (ed. F. Durst *et al.*), pp. 3.33–3.38. Springer. (Also *SANDIA rep.* SAND84–8940.)

MASLOWE, S. A. 1977 Weakly nonlinear stability theory of stratified shear flows. *Q. J. Roy. Met. Soc.* **103**, 769–783.

MONKEWITZ, P. A. 1982 On the effect of the phase difference between fundamental and subharmonic instability in a mixing layer. *Internal rep., Univ. of California, Los Angeles.*

MONKEWITZ, P. A. 1983 On the nature of the amplitude modulation of jet shear layer instability waves. *Phys. Fluids* **26**, 3180–3184.

MONKEWITZ, P. A. & HUERRE, P. 1982 The influence of the velocity ratio on the spatial instability of mixing layers. *Phys. Fluids* **25**, 1137–1143.

PATNAIK, P. C., SHERMAN, F. S. & CORCOS, G. M. 1976 A numerical simulation of Kelvin–Helmholtz waves of finite amplitude. *J. Fluid Mech.* **73**, 215–240.

PIERREHUMBERT, R. T. & WIDNALL, S. E. 1982 The two- and three-dimensional instabilities of a spatially periodic shear layer. *J. Fluid Mech.* **114**, 59–82.

REDEKOPP, L. G. 1977 Solitons in shear flows. *Proc. NSF Reg. Conf. in the Math. Sciences on Geofluiddynamical Wave Maths* (ed. W. O. Criminale), pp. 202–215. University of Washington, Seattle.

RILEY, J. J. & METCALFE, R. W. 1980 Direct numerical simulation of a perturbed turbulent mixing layer. *AIAA paper* 80–0274.

ROBINSON, J. L. 1973 Stability of inviscid shear layer which is periodic in space. *N.Z. J. Sci.* **16**, 903–908.

SMITH, F. T. & STEWART, P. A. 1987 The resonant-triad nonlinear interaction in boundary-layer transition. *J. Fluid Mech.* **179**, 227–252.

STUART, J. T. 1960 On the nonlinear mechanics of wave disturbances in stable and unstable parallel flows. Part 1. *J. Fluid Mech.* **9**, 353–370.

STUART, J. T. 1967 On finite amplitude oscillations in laminar mixing layers. *J. Fluid Mech.* **29**, 417–440.

WATSON, J. 1960 On the nonlinear mechanics of wave disturbances in stable and unstable parallel flows. Part 2. *J. Fluid Mech.* **9**, 371–389.

WEHRMANN, O. & WILLE, R. 1958 Beitrag zur Phänomenologie des laminar–turbulenten Überganges bei kleinen Reynoldszahlen. *Grenzschichtforschung*, pp. 387–403. Springer.

ZAMAN, K. B. M. Q. & HUSSAIN, A. K. M. F. 1980 Vortex pairing in a circular jet under controlled excitation. Part 1. General jet response. *J. Fluid Mech.* **101**, 449–491.